AD NUMBER

ADB183345

NEW LIMITATION CHANGE

TO
Approved for public release, distribution
unlimited

FROM
Distribution: DTIC users only.

AUTHORITY

NRL ltr, 25 Jan 2001.

5

AD-B183 345

NRL Report 4600

ADVANCES IN THE PHYSICS
OF THE UPPER AIR SINCE 1950

E. O. Hulburt

Director of Research

COPY 1

October 25, 1955

DTIC
ELECTE
APR 19 1994
S B D

94-11524

94 4 15 084

CONTENTS

1

ABSTRACT

The report describes progress which has been made since about 1950 in investigating the upper atmosphere. Important data up to great heights were obtained by means of instruments on rockets. The vertical distribution of atmospheric density was measured to 219 km, of pressure to 130 km, of ozone to 70 km, and of electron density of 219 km. In a daytime flight O_2, O, N_2, and N were observed from 98 to 137 km; O_2 was observed to be more than 60 percent dissociated from 110 to 128 km. The ratio A/N_2, argon to molecular nitrogen, was found to be about the same from 110 to 137 km as at ground level.

Positive ions of atomic masses 16, 26, 30, and 32, identified as O^+, CN^+, NO^+, O_2^+, respectively, were observed in a daytime flight from 94 to 124 km. In a night flight only N_2^+ was recorded from 97 to 114 km.

From an altitude above 100 km the solar spectrum was photographed into the vacuum ultraviolet to 970A, and was recorded with photocells in the soft x-ray region from 100A to 6A. At about 2090A the character of the spectrum changed abruptly, the energy decreased sharply, the Fraunhofer absorption lines disappeared and at shorter wavelengths gave way to emission lines.

The vertical distribution of ozone was measured to 70 km, and a quantitative theory of ozone formation was worked out. Calculation indicated that the temperature maximum at about 50 km was due to the absorption of solar ultraviolet energy by ozone.

The various facts of the ionosphere were gathered together in a theory which attributed the cause of the normal D region to solar hydrogen Lyman α, 1216A, of normal E region to x-rays below 100A, and of F2 to ultraviolet light in the thus far unobserved spectrum from 200A to 600A. No explanation of F1 was made. Anomalies in D ionization appeared to be due to enhanced bursts of solar x-rays, and sporadic E appeared to be blobs of ionization caused by meteors.

A working model atmosphere based on the observed pressure, density, and composition was drawn up and extrapolated to 500 km. Its temperature increased rapidly from $200^{\circ}K$ at 100 km to $1043^{\circ}K$ at 200 km, and $1100^{\circ}K$ at 300 km; the temperature was calculated to agree with the energy supplied by the ionosphere and heat conduction downward.

From the observed changes in the ionosphere over two solar cycles, the solar intensity in the wavelengths which cause E, F1, and F2 was calculated to increase by a factor of about 2.3 from sunspot minimum to maximum.

Better spectra and better analysis of the spectra removed much confusion about the auroral spectrum. Doppler broadened $H\alpha$ was discovered in the quiet auroral arc at the commencement of an auroral display, and was interpreted to mean that the display was initiated by solar protons of speed greater than 300 km per sec entering the upper atmosphere. A new theory of the aurora was outlined based on magnetically self-focused proton streams from the sun.

ADVANCES IN THE PHYSICS OF
THE UPPER AIR SINCE 1950

1. INTRODUCTION

This report is based on a chapter which was prepared for a forthcoming publication entitled "Meteorological Research Review," edited by James E. Miller and published by the American Meteorological Society. The report, which describes progress made during the past five years in investigating the upper atmosphere, provides much data and general interest for students of this subject. It is of particular interest to the Naval Research Laboratory, where so many of the contributions have originated.

On the experimental side, major advances have been made by means of instruments carried to great heights on rockets from which the vertical distribution of the atmospheric density was measured to 219 km, of the pressure to 130 km, of ozone to 70 km, and of the electron density to 219 km. Data were obtained on oxygen dissociation to 128 km, composition of the air to 137 km, and O^+ and O_2^+ to 124 km. By means of optical spectrographs, and of photon counters for ultraviolet and x-ray, many features of the solar spectrum nearly outside the atmosphere in the region from 3000A to 6A have been observed and measured, leaving, however, an unexplored gap in the important region from about 970A to 100A.

As a result, probably many of the important facts of the atmosphere up to 130 km may be considered to be known and understood. From 130 to 219 km, less is known; and above this, one is almost entirely in a region of extrapolation. However, the extrapolation is less extensive, starting as it does more or less from 219 km, than it used to be when 20 km was the starting point.

It is now possible to attribute with some justification the cause of the D region of the ionosphere to the solar Lyman α line at 1216A, and of the E region to solar x-ray or short ultraviolet light from 10A to 100A. The cause of F1 remains obscure. Although the F2 region is entirely above 219 km, and hence in the extrapolation altitudes, a plausible explanation of this region is now available based on solar ultraviolet light around 200A and recombination by charge exchange.

By means of spectrographs on the ground, protons were discovered entering the high atmosphere during the incipient period of an auroral display. A new theory of the aurora was outlined based on magnetically self-focused proton streams emitted from the sun.

No new facts about magnetic storms have come to light. The nature of the emanation from the sun which causes the majority of the ionospheric and magnetic disturbances remains unknown, and the manner in which it gives rise to the disturbances is not understood. But perhaps the stage is being set for future progress in these stubborn problems.

2. THE PRESSURE, DENSITY, AND TEMPERATURE
OF THE UPPER ATMOSPHERE

The investigation of the atmosphere to great heights has been carried on in the United States since 1946 by means of instruments on rockets. Altogether over 200 rockets have been fired by various agencies for the purpose of upper air research, and more than half of these have carried many types of instruments for measuring the pressure, density, and

1

other fundamental data of the atmosphere. In Table 1 and Figs. 1 and 2 are listed the values of the pressure, p, (millimeters of mercury) and the density, ρ, (grams per cubic meter) up to an altitude of 220 km. These are the smoothed, averaged values obtained by the Naval Research Laboratory from all rocket flights at White Sands, New Mexico, up to July 1954.[1] Values of p were observed up to 128 km, and the values in Table 1 and Fig. 1 above this were extrapolated; ρ was observed up to 219 km. The probable errors in p and ρ were less than 10 percent for altitudes below 75 km, but increased with altitude to a factor of 2 or 3 at 200 km. The two most prominent sources of systematic error were rocket yaw and out-gassing, the latter tending to cause too high values of ρ. An indication of this was the fact that solar soft x-ray measurements at altitudes from 110 to 128 km led to pressures about one third of those of Table 1 (see section 7).

TABLE 1
Atmospheric Pressure, Density,
and Temperature from Rocket Measurements

Altitude (km) (1)	Pressure (mm of Hg) (2)	Density (grams m^{-3}) (3)	Temperature (^{0}K)	
			$\mu = 29$ (4)	$\mu = 29$ to 20 (5)
0	760	1250	290	290
10	203	420	230	230
20	48.5	92	210	210
30	9.5	19	235	235
40	2.4	4.3	260	260
50	7.5×10^{-1}	1.3	270	270
60	2.1×10^{-1}	3.8×10^{-1}	260	260
70	5.5×10^{-2}	1.2×10^{-1}	210	210
80	1.0×10^{-2}	2.5×10^{-2}	190	190
90	1.8×10^{-3}	4.0×10^{-3}	210	210
100	4.0×10^{-4}	8.3×10^{-4}	240	230
110	1.0×10^{-4}	2.0×10^{-4}	280	260
120	3.8×10^{-5}	4.9×10^{-5}	330	300
130	1.4×10^{-5}	1.7×10^{-5}	390	340
140	7.4×10^{-6}	5.8×10^{-6}	450	380
150	3.6×10^{-6}	2.8×10^{-6}	520	430
160	1.9×10^{-6}	1.5×10^{-6}	600	480
170	1.3×10^{-6}	8.0×10^{-7}	620	510
180	7.8×10^{-7}	5.1×10^{-7}	690	540
190	4.7×10^{-7}	3.1×10^{-7}	740	550
200	3.2×10^{-7}	2.1×10^{-7}	770	550
210	2.0×10^{-7}	1.4×10^{-7}	790	560
220	1.3×10^{-7}	1.0×10^{-7}	820	570

For a gas the relation between pressure, p, absolute temperature, t^0K, and the density, ρ, is given by the equation of state,

$$p = \rho kt/\mu, \qquad (1)$$

where μ is the mass of the average gas molecule and k is the Boltzmann constant. If the gas is composed of molecules of masses m_1, m_2, m_3, . . ., and if the number of such particles
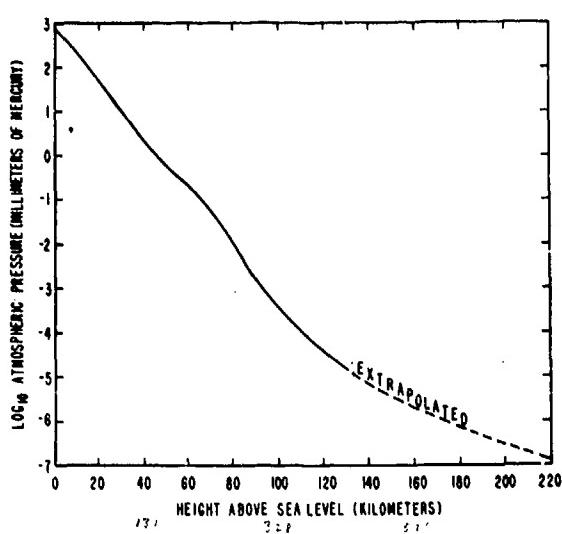
Fig. 1 - Atmospheric pressure from
rocket data
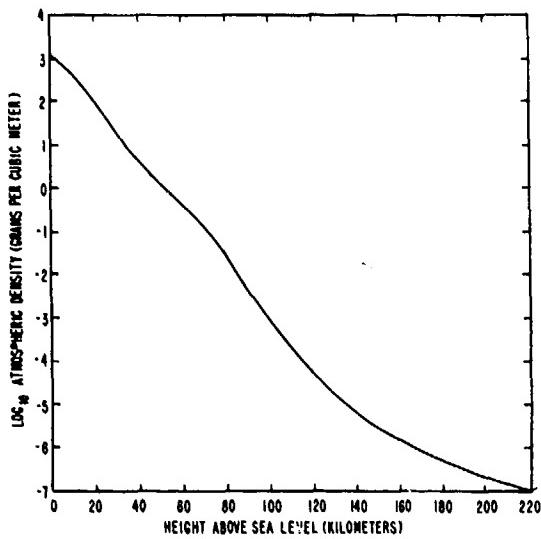
Fig. 2 - Atmospheric density from
rocket data

per unit volume is n_1, n_2, n_3, ..., respectively, then

$$\rho = n_1 m_1 + n_2 m_2 + n_3 m_3 + \cdots, \tag{2}$$

and

$$\mu = \rho/(n_1 + n_2 + n_3 + \cdots). \tag{3}$$

If the gas is in equilibrium in the gravitational field, g, of the earth, the change in pressure with change in altitude, h, is expressed by the barometric equation dp = -ρg dh, which may be written

$$\rho = -\frac{1}{g} \frac{dp}{dh}, \tag{4}$$

or

$$p = -\int \rho g \, dh. \tag{5}$$

In general, g is a function of h. From Eq. (4), ρ may be calculated from the slope of the p-h curve, and from Eq. (5) p may be calculated from the integral of the ρ-h curve. The curves of Figs. 1 and 2 and the values of Table 1 resulted from drawing smooth curves through the observed points and then adjusting the curves until both Eqs. (4) and (5) were satisfied simultaneously. Since p was observed only to 128 km, the p-h curve was continued to 220 km by the use of Eq. (5) and the observed values of ρ up to 220 km.

The temperature, t, was calculated from the values of p or ρ of Figs. 1 and 2 by means of Eq. (1) and assumed values of μ; the values of t are in columns (4) and (5) of Table 1, and the t-h curves are plotted in Fig. 3, curves 1 and 2. Column (4) was obtained by assuming μ to be the same at all altitudes and equal to 29 atomic hydrogen masses, which is approximately the value at sea level. Column (5) was obtained by assuming μ to be 29 from 0 to 80 km and then to decrease linearly to 20 at 200 km, as would be the case if the dissociation of oxygen and nitrogen molecules to atoms started at 80 km and increased with altitude. Qualitatively, rocket observations indicated that atoms existed above 97 km; this
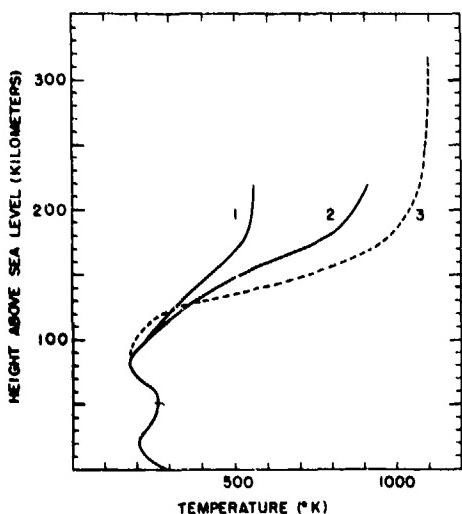
Fig. 3 - Atmospheric temperature
calculated from rocket pressure and
density data, curves 1 and 2; adjusted
for thermal conductivity, curve 3.

was favorable to column (5). However, since
the amount of dissociation has not been deter-
mined exactly, the temperatures above 100 km
cannot be said to be known with precision at the
present time.

In 1952 the Rocket Panel published[2] tables
of upper air pressures, densities, and temper-
atures up to 220 km based on all rocket data to
January 1952. The tables agree with Table 1
within 10 percent, which is well within the accu-
racy of the data, and hence any differences
between the tables is without significance.

The upper air values of p and ρ made at
White Sands, New Mexico, on which the values
of Table 1 are based, covered all seasons of the
year, and showed no clear-cut evidence of a
seasonal effect. Also, p and ρ data were obtained
from rockets at the equator and at three differ-
ent places in the Baffin Bay area (70° N lat.,
west of Greenland), and the results were the
same as at White Sands. Therefore, although
it seemed reasonable to think that there must
be a geographical variation of p and ρ,
any effect of this kind was less than the error
of measurement, and has yet to be revealed.

That the atmosphere must be well mixed from sea level up to 130 to 150 km was first
shown by Maris[3] in a brilliant argument in 1928. His method was simply to assume that
the atmosphere was completely mixed and then to calculate how long it would take the lighter
gases to diffuse upward and the heavier ones downward. The rate of diffusion depended on
the pressure (as well as on t and μ), and it turned out that the time for diffusive separation
to be established was about 5 days at 130 km and increased rapidly with decreasing altitude.
Therefore, except for the possibility of the dissociation of molecules to atoms and the for-
mation of compounds as ozone and oxides of nitrogen, it was concluded that, since some
vertical wind stirring must exist, the composition of the atmosphere must be approximately
unchanged from sea level to about 150 km. This conclusion was later supported by a wide
variety of observations on clouds, smoke trails, balloons, meteor trains, and ionosphere
motions which indicated much wind stirring up to at least 120 km. Further corroborative
evidence came from a recent rocket measurement of the ratio of argon to nitrogen, described
in section 3, which showed that the ratio A/N_2 was about the same from 110 to 137 km as
at ground level.

Table 2 was drawn up as a working model of the atmosphere. It incorporates certain
small changes in Table 1 and provides extrapolation to an altitude of 500 km. It assumes
the temperature distribution given by curve 3, Fig. 3, which indicates a temperature about
30° lower than that of Table 1 at 100 km, and a rapid increase above 130 km to 1100°K at
300 km in the high isothermal region. The density of Table 2 is about 0.45 of that of Table 1
at 110 km, in accord with the x-ray measurement of section 7. Above 100 km the percentage
compositions of O_2, O, N_2, and N were assumed as given in the last four columns of the table,
and the particle densities of these gases for the temperatures shown in column (2) were
calculated for equilibrium with gravity, and were extrapolated to 500 km. The particle
densities were added at each level to give the total particle density of column (3). Gases
other than oxygen and nitrogen comprise less than 3 percent of the atmosphere and are not
included in Table 2. The dissociation of O_2 of columns (5) and (6) was based on evidence
described in section 7.

TABLE 2
Model Atmosphere Extrapolated to High Altitudes

Altitude (km) (1)	Temperature (°K) (2)	Particle Density, n (3)	Particle Mass (4)	Percentage Composition			
				O_2 (5)	O (6)	N_2 (7)	N (8)
0	290	2.5×10^{19}	28.8	21	0	79	0
10	230	8.7×10^{18}					
20	210	1.9×10^{18}					
30	235	3.9×10^{17}					
40	260	8.9×10^{16}					
50	270	2.4×10^{16}	28.8	21	0	79	0
60	245	7.4×10^{15}					
70	210	2.0×10^{15}					
80	185	4.1×10^{14}					
90	183	6.6×10^{13}	28.8	21	0	79	0
100	200	1.1×10^{13}	28.8	20	1	79	0
110	230	2.0×10^{12}	27.0	11	14	75	0
120	280	5.1×10^{11}	25.3	7	24	69	0
130	423	2.1×10^{11}	25.2	6	25	69	0
140	594	5.8×10^{10}	25.0	5	26	69	0
150	737	3.0×10^{10}	24.5	5	26	65	4
160	846	1.9×10^{10}	23.7	4.4	28	60	7.6
170	925	1.3×10^{10}	23.0	3.9	32	55	9.1
180	979	9.3×10^{9}	22.3	3.3	35	50	11.7
190	1017	7.0×10^{9}	21.7	2.8	39	46	12.2
200	1043	5.4×10^{9}	21.1	2.5	44	41	12.5
220	1074	3.4×10^{9}	20.0	1.8	51	34	13.2
240	1088	2.3×10^{9}	19.2	1.3	56	27	15.7
260	1095	1.6×10^{9}	18.2	0.9	60	20	19.1
280	1098	1.1×10^{9}	17.5	0.7	65	15	19.3
300	1100	7.7×10^{8}	16.8	0.5	67	10	22.5
350	1100	3.5×10^{8}	16.3	0.2	68	7	24.8
400	1100	1.5×10^{8}					
450	1100	5.9×10^{7}					
500	1100	3.1×10^{7}					

The evidence for the dissociation of N_2 of columns (7) and (8) was mainly theoretical; some slight experimental evidence appears in section 3. The increase in temperature above 200 km was chosen to satisfy the condition that the loss of heat energy by conduction downward would be about the same as the energy received from the absorption of solar ultraviolet and infrared light in the high levels, as explained in section 13. Therefore, although the atmospheric model of Table 2 has not been checked by direct experiment above 200 km, it illustrates an attempt to satisfy a number of fundamental requirements.

3. MASS SPECTROGRAPH AND POSITIVE-ION SPECTROGRAPH MEASUREMENTS WITH ROCKETS

A mass spectrograph[4] and a positive-ion spectrograph[5] were flown successfully on rockets at White Sands, New Mexico. Certain of the results, described below, seemed trustworthy, but the flights were not perfect and obviously a repetition was necessary. Further experiments were scheduled for July 1955. In pioneer experiments of this kind, which are of great difficulty, one can never be satisfied with a single experiment even if everything should appear to work perfectly. The mass spectrograph was on Aerobee NRL-13 which was fired 9 minutes after midnight on February 12, 1953, and reached an altitude of 137.3 km. The instrument was designed to record atomic mass units (AMU) from 6 to 54 AMU in gas pressures below about 5×10^{-4} mm of mercury, or at altitudes above about 95 km. The rocket was a very light-weight and high-powered rocket and became unusually hot during its powered flight as evidenced by burnt paint on the nose section. Twenty-three peaks were on the mass spectrograph records in the altitude range from 98 to 137.3 km. Five of these, listed in Table 3, were believed to be due to atmospheric gases because they were repeated symmetrically on both the upward and downward legs of the flight. The other 18 peaks were unsymmetrically or erratically distributed throughout the flight and were probably, some or all, due to rocket gases and not to the ambient air. The presence of atomic oxygen and atomic nitrogen at these levels (Table 3) was noteworthy.

TABLE 3
Mass Spectrograph Data
(Altitude Range of 98 to 137.3 km)

Mass Number (AMU)	Identification
40	Argon A
32	Oxygen O_2
28	Nitrogen N_2
16	Oxygen O
14	Nitrogen N

The ratio A/N_2, argon to molecular nitrogen, was about the same from 110 to 137.3 km as at ground level. This, as has been said, indicated that there was no diffusive separation of the atmospheric gases. The ratio N/N_2 was of order 10^{-2} and the ratio O/O_2 was uncertain; since a portion of the atomic nitrogen and oxygen was produced in the mass spectrograph, these ratios gave no trustworthy indication of the amounts of N and O in the ambient atmosphere.

The positive-ion spectrograph was carried to 219 km by Navy Viking rocket No. 10 on May 7, 1954, at 10 o'clock in the morning,[5] and gave good records at almost every kilometer on the upward flight from 93 to 219 km. Because of rocket vicissitudes (a small explosion, a roll, and ejection of oxygen fuel), confused data were obtained on the descent. The data are summarized in Table 4, and the original records for four heights are shown in Fig. 4. Essentially the records showed that the region from 94 to 124 km contained O_2^+, O^+, CN^+, and NO^+. At about 124 km, CN^+ and NO^+ weakened to indistinguishability, and thereafter there was no further change, O_2^+ and O^+ remaining strong to the top of the flight. The fact that both O_2^+ and O^+ were observed up to 219 km was of great importance in the theory of the ionosphere (section 8).

TABLE 4
Positive-Ion Spectrograph Data
(Altitude Range of 94 to 219 km)

Altitude (km)	Strong Peaks (AMU)	Weak Peaks (AMU)	Identification
94 to 124		12*	C^+
	16*		O^+
		18*	H_2O^+
		19*	F^+ (?)
		21	?
		23	Na^+
	26*		CN^+
	30*		NO^+
	32*		O_2^+
		38*	?
		45	?
124 to 219	16*		O^+
	32*		O_2^+

*Peaks of these mass numbers were detected in the mass spectrograph experiment, Reference (4)

The identification of the positive ions given in Table 4 seemed reasonable with the possible exception of the strong peak at 26 AMU, which was ascribed to CN^+. It seemed surprising that there was enough carbon at such a high altitude to give a strong yield of CN. The explanation was offered that the carbon might come from meteors. The absence of peaks at 14 and 28 AMU due to N^+ and N_2^+ seemed strange.

Note added July 28, 1955. The ion spectrograph experiments scheduled for July 1955 were accomplished successfully on an Aerobee rocket on July 8, which reached an altitude of 115 km. The flight was at 1:40 A.M. and the rocket carried two spectrographs, one for positive ions and one for negative ions. Through the altitude range of 90 to 115 km, N_2^+ was recorded strongly and clearly on both the
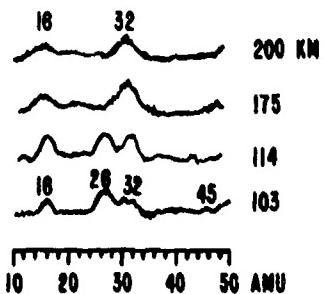
Fig. 4 - Samples of ion spectrograph records.

upward and downward legs of the flight, and no other ions of either sign were detected. The sensitivity was such that other ions would have been detected if their concentration had been as much as one percent of that of $N_2{}^+$. No magnetic or solar disturbance was in evidence at the time. Further experiments were planned for November, 1955. This result, being at night, resolves none of the daytime questions. It merely brings up new questions about the night ionization. For example, are there no negative ions, or are there negative ions in some other levels than 90 to 115 km?

4. SPECTRUM OF THE SUN OUTSIDE OF THE ATMOSPHERE

The spectrum of the sun is of two-fold interest because it gives information about the physical state of the emitting and absorbing layers of the outer atmosphere of the sun, and because it causes heating, ionization, and chemical changes in the outer atmosphere of the earth. In a series of very beautiful experiments with rockets nearly outside the atmosphere the spectrum of the sun was photographed[6] in the ultraviolet as far as 977A, and was measured with photon counters[7] in the ultraviolet as far as 1100A and in the soft x-ray region from about 100A to 6A.

No attempt is made to give here the detailed analysis of the (relatively) high dispersion spectra in which over 1000 lines in the solar spectrum below 3000A were identified.[8] That would be appropriate to an astrophysical report rather than to a geophysical one as this. In Fig. 5 is given the solar energy curve outside the atmosphere from 3400A to 2000A. The curve is the weighted average of about 15 curves obtained from 7 different spectrographs flown in six rockets over the years 1949 to 1952.[6] The curve from 2200A to 2000A was extrapolated because the energy standardization was obtained by comparison with a carbon arc which was calibrated only to 2200A (work is nearly completed which will extend the calibration to 1700A). It is seen that the curve falls below the 5500°K black body curve by factors of about 3 and 15 at 2500A and 2000A, respectively. Photon-counter measurements at about 1450A and 1250A indicated equivalent black body temperatures of 4050° and 3900°K, respectively.
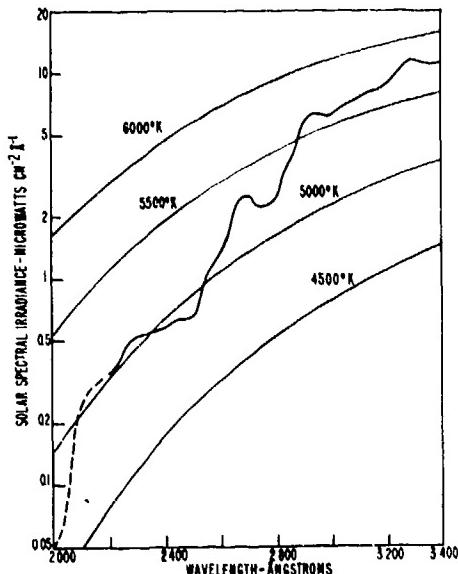

Fig. 5 - Solar spectral irradiance outside the earth's atmosphere, averaged over 100A intervals.

In Fig. 6 is given the complete solar energy curve outside the atmosphere, the portion below 3000A coming from Fig. 5. From this curve the solar constant, i.e., the solar energy falling on the "top" of the earth's atmosphere, was calculated to be 2.00 ±0.04 cal cm^{-2} min^{-1}, or 1.35 ±0.027 × 10^6 erg cm^{-2} sec^{-1}, which is believed to be the most authoritative value available at the present time. The value referred to the mean solar distance and any variance throughout a solar cycle, if it existed, was within the probable error.

In Fig. 7 is shown the best rocket solar spectrum in the vacuum ultraviolet yet obtained.[9] It was photographed from an Aerobee rocket on February 21, 1955, near the top of the flight at an altitude of 117 km above New Mexico with an exposure of 30 seconds by means of a simplified type of sun follower. Densitometer traces of the spectrum of Fig. 7 are shown in Figs. 8 and 9. The abrupt, and unexpected, change in the character of the solar spectrum at about 2090A is clearly seen in Fig. 8. At this wavelength the average energy level suddenly falls and the Fraunhofer absorption lines almost completely disappear. It seems reasonable to attribute this change to a sudden increase in the opacity of the solar atmosphere, and to think that for wavelengths below 2090A the radiation comes from a higher level where the temperature is lower. The increase in opacity may be due to the ionization of some abundant elements such as aluminum and calcium.
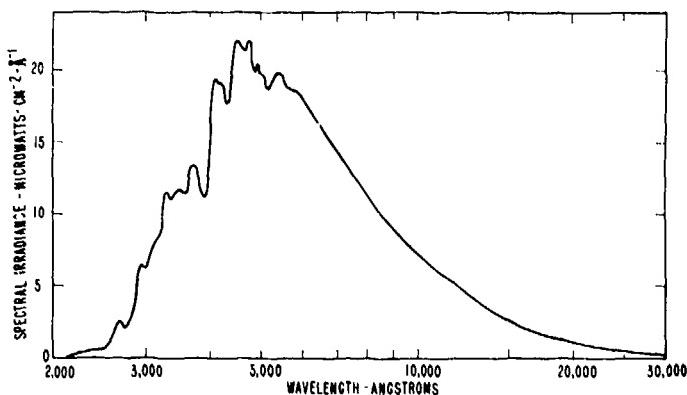
Fig. 6 - The complete solar spectral irridiance curve
from 2300A to 30,000A
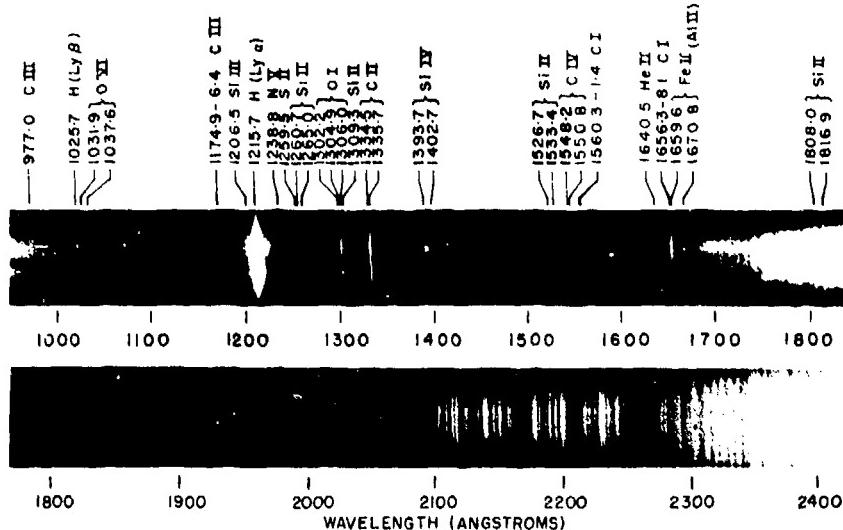
Fig. 7 - Ultraviolet solar spectrum photographed at
117 km above New Mexico on February 21, 1955
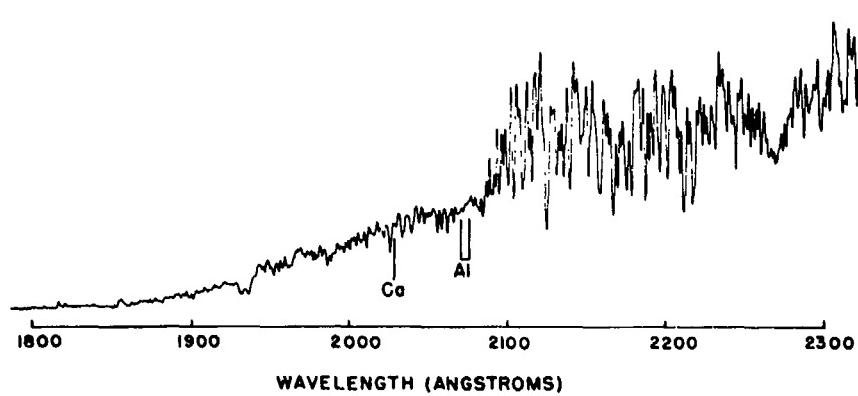
Fig. 8 - Densitometer trace of long wave portion of the
solar spectrum of Fig. 7
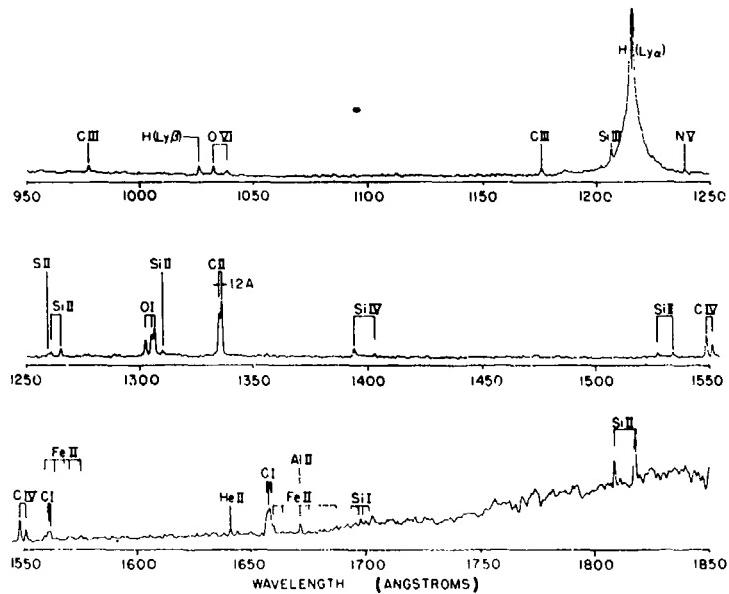
Fig. 9 - Densitometer trace of short wave portion
of the solar spectrum of Fig. 7

Below 2000A the absorption lines gave way to emissions, the last absorption feature being identified as a Si I multiplet near 1680A. As seen in Fig. 7, the emission lines were produced by atoms up to 5 times ionized. The greatly overexposed line at 1215.7A is the Lyman α line of hydrogen, and the more moderately exposed line at 1025.7A is the Lyman β line. The great intensity difference between Lyman α and β is believed to be due largely to atmospheric absorption, because the spectrograph speed changed only by a factor of two between these wavelengths. The shortest line which was observed was a C III line at 977.0A. Lymn γ, which would occur at 972A, falls on a strong atmospheric nitrogen absorption line and could not get down to 117 km.

By means of photon counters sensitive in the wavelength band 1000 to 1300A on three Aerobee rockets fired in May, 1952, it was found that Lyman α was a narrow line, less than 0.5A wide, of energy 0.1 erg cm^{-2} sec^{-1} and that the intensity of the continuum in this band was less than 0.01 erg cm^{-2} sec^{-1}, and hence was small compared to the intensity of Lyman α itself; the continuum energy corresponded to a black body at a temperature less than $4050°K$.

Solar radiation in the soft x-ray region of the spectrum was measured by means of photon counters in six rockets; the results are listed in Table 5. Except for the last rocket, Aerobee 16, all the measurements consisted of sampling only one band of the x-ray spectrum. In the case of Aerobee 16 three wavelength bands were covered, and the observed distribution of energy in these three bands indicated a coronal emission temperature of $750,000°K$. The sun was extremely quiet at the time. It is seen from Table 5 that there was considerable variation in the intensity of the x-rays in the shorter wavelength bands; an extreme variation was in the band 8A-20A of Viking 9 and Aerobee 16. It was believed that the variation was due to solar changes. To bring this out there were listed in Table 5 the intensities of the coronal line 6701.83A, due to Ni XV, derived from the coronagraph records of Sacramento Peak Observatory, New Mexico. It is seen that when the line was strong, indicating solar activity, as for Viking 9, the 8A-20A x-rays were strong, and when the line was weak, as for Aerobee 14 and 16, the x-rays were weak.

TABLE 5
Solar X-Ray Energy Outside the Atmosphere
and Coronal Line Intensity

Date	Rocket	X-Ray Band (A)	Energy (erg cm^{-2} sec^{-1})	Ni XV Relative Intensity
9/29/49	V2 49	8-10	10^{-4}	--
5/1/52	Aerobee 9	6-7	4×10^{-4}	26
5/5/52	Aerobee 10	6-7	10^{-5}	32
12/15/52	Viking 9	8-20	0.2-0.6	25
11/15/53	Aerobee 14	8-20	3×10^{-3}	0.5
12/1/53	Aerobee 16	8-20	2×10^{-3}	0
		44-60	3×10^{-2}	0
		60-100	2×10^{-2}	0

In the foregoing experiments the solar spectrum was observed throughout the ultraviolet down to 977A, and in the x-ray region from 100 to 6A. There were no observations in the vacuum ultraviolet from 977A to 100A. This is an extremely important region, for these wavelengths are probably the principal cause of ionization and photochemical reactions in the gases of the upper atmosphere. The importance of attempting to observe this region was fully realized and further rocket experiments were planned. The experiments promise to be very exacting, because of the difficulty of eliminating scattered longer wavelength light from photographed spectra, and the necessity of using windowless photon tubes as there are no window materials in this region. The rocket must carry the spectrograph or photon tube well above 200 km in order to get above the air absorption.

5. THE VERTICAL DISTRIBUTION OF
   ATMOSPHERIC OZONE

The vertical distribution of ozone in the atmosphere has been measured directly 5 times by means of 3 rockets equipped with spectrographs and 2 rockets with photon counters.[10] The results are given in Fig. 10 and refer to the atmosphere above New Mexico. Two of the flights were made with the sun at a low altitude to determine the concentration of ozone to as high an altitude as possible, in order to explain the temperature maximum near 50 km produced by the absorption of ultraviolet sunlight by ozone and to serve as a guide in the theory of ozone formation. These flights were on June 14, 1949, and January 25, 1951, the solar altitude being about 1° and 10°, respectively. The curves for these two flights extended to about 70 and 65 km and are shown on an expanded scale in Fig. 10. The ozone concentration from the June 14 measurements are given in Table 6. At lower altitudes the January 25 curve gave the lowest ozone concentration of any of the determinations, and in order to include a reasonable amount of total ozone in the atmosphere, its peak concentration must have been as low as 10 or 15 km. This is not impossible although it may be unusual. Two more ozone rocket flights are planned for 1957 for the sake of repetition and to test whether the differences in the upper portions of the curves of Fig. 10 are real.
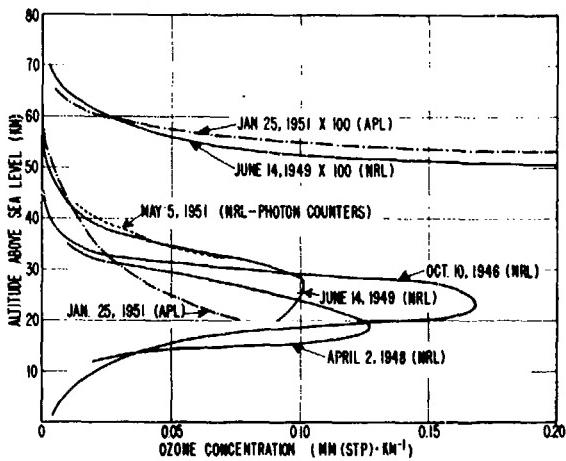
Fig. 10 - Ozone determinations from rockets

On the spectra of the June 14 flight no features were observed up to 70 km that could not be accounted for by ozone absorption, and between 70 and 110 km there were no differences between the spectra. Thus no gases other than ozone, such as the oxides of nitrogen, were detected in this altitude range. The NO^{+} which was observed with the ion spectrograph (section 3) was apparently in too low concentration to be revealed by the spectra.

The photochemical theory of the formation of ozone by sunlight in the upper atmosphere has been studied by a number of investigators. The most recent and complete theory was that of Johnson et al,[11] which made use of the usual reactions of oxygen and ozone with solar ultraviolet light. The more important reactions were assumed to be

$$O_2 + h\nu \rightarrow O + O \qquad (J_2)$$

$$O_3 + h\nu \rightarrow O_2 + O \qquad (J_3)$$

$$O + O + M \rightarrow O_2 + M \qquad (k_1)$$

$$O + O_2 + M \rightarrow O_3 + M \qquad (k_2)$$

$$O + O_3 \rightarrow 2O_2 \qquad (k_3)$$
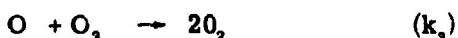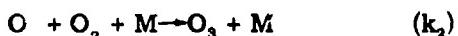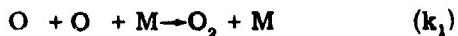
TABLE 6
Ozone Concentration Above New Mexico,
June 14, 1949

Altitude Above Sea Level (km)	Ozone Concentration (mm(STP)/km)	Altitude Above Sea Level (km)	Ozone Concentration (mm(STP)/km)
20	9.1×10^{-2}	46	6.4×10^{-3}
22	9.6×10^{-2}	48	3.2×10^{-3}
24	9.9×10^{-2}	50	2.2×10^{-3}
26	1.08×10^{-1}	52	1.3×10^{-3}
28	1.03×10^{-1}	54	7.4×10^{-4}
30	8.9×10^{-2}	56	5.1×10^{-4}
32	7.5×10^{-2}	58	3.6×10^{-4}
34	5.7×10^{-2}	60	3.0×10^{-4}
36	3.9×10^{-2}	62	1.9×10^{-4}
38	2.5×10^{-2}	64	1.2×10^{-4}
40	1.6×10^{-2}	66	6.5×10^{-5}
42	1.2×10^{-2}	68	3.8×10^{-5}
44	9.4×10^{-3}	70	2.5×10^{-5}

where J_2 and J_3 were the rates of dissociation per unit concentration of O_2 and O_3, respectively, and k_1, k_2, and k_3 were the respective coefficients of collision. Rate J_2 depended on the intensity of sunlight and the absorption cross section of O_2 in the Schumann continuum, and J_3 depended on similar quantities of O_3 in the Hartley band. At the present time the solar intensity in the Schumann region below 2200A and the absorption cross section of O_3 below 2400A are not well known. The coefficients k_1, k_2, and k_3 were obtained by extrapolation from laboratory chemical reaction measurements made at higher pressures than those of the atmosphere above 30 km. For these reasons the theoretical calculations were not carried above 90 km. Assuming photochemical equilibrium, one has

$$2 J_2 n_2 + J_3 n_3 - 2 k_1 n_1^2 n - k_2 n_1 n_2 n - k_3 n_1 n_3 = 0 \qquad (6)$$

and

$$J_3 n_3 - k_2 n_1 n_2 n + k_3 n_1 n_3 = 0, \qquad (6a)$$

where n_1, n_2, n_3, and n are the particle densities of O, O_2, O_3, and the third body, M, respectively. M was assumed to be any air particle, hence n was the total particle density obtained from column (3), Table 2, below 100 km the density of oxygen molecules, n_2, was approximately 0.21 n, and is given in Table 7. The values of n_3 and n_1 were calculated from Eqs. (6) and (6a) shown in Table 7. The values of n_3 were plotted in the theoretical curve of Fig. 11 and agree well with the observed curve of June 14, 1949, above 40 km; it departed from the observed curve below 40 km. It was seen from the theoretical calculation that at altitudes from 50 to 90 km photochemical equilibrium was established in minutes or seconds, and therefore agreement of theory and observation might be expected in this region. Below 35 km, however,

TABLE 7
Particle Density of O_2, O_3, and O

Altitude (km)	n_2 (number cm^{-3})	n_3 (number cm^{-3})	n_1 (number cm^{-3})
30	8.2×10^{16}	6.7×10^{12}	1.7×10^6
40	1.9×10^{16}	4.8×10^{11}	2.0×10^{10}
50	5.0×10^{15}	4.3×10^{10}	4.4×10^{10}
60	1.6×10^{15}	7.0×10^9	1.0×10^{11}
70	4.2×10^{14}	1.2×10^9	1.9×10^{11}
80	8.6×10^{13}	7.6×10^7	2.7×10^{11}
90	1.4×10^{13}	5.0×10^6	3.3×10^{11}
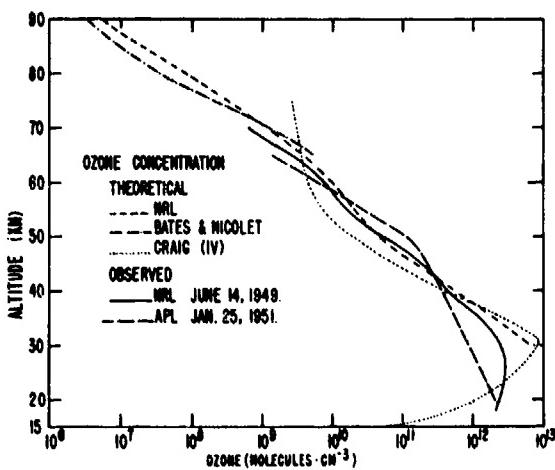
Fig. 11 - Comparison of ozone observations and theory

photochemical equilibrium was established very slowly, requiring days. Therefore, in this region one would not expect agreement with theory, because winds, effects of dust and water vapor, and other things not contemplated in the simple photochemical theory interfere with the establishment of equilibrium conditions.

Table 7 shows that the dissociation of oxygen was very small in the lower levels and increased with altitude to about 2.4 percent at 90 km. This was a by-product of the ozone formation theory.

It is of interest, although perhaps somewhat out of place here, to mention the manner in which ozone has recently been shown to affect the color of the sky.[12] During the day the clear sky is blue because of Rayleigh scattering by the air molecules, and ozone has little effect on the color. But near sunset and throughout twilight, ozone colors the sky profoundly. For example, in the absence of ozone the zenith sky would be a grayish green at sunset becoming yellow or tawny in twilight, but with ozone the zenith sky is blue at sunset and remains blue throughout twilight (as is observed), the blue at sunset being due about 1/3 to scattering and 2/3 to ozone, and during twilight wholly to ozone.

6. UPPER ATMOSPHERIC TEMPERATURE CHANGES
DUE TO OZONE

The rapid decrease of the temperature of the atmosphere with altitude in the first 8 to 15 km of the lower atmosphere, from the surface to the stratosphere, has been thoroughly discussed in treatises on meteorology. It was shown quantitatively to be the adiabatic lapse rate caused by vertical stirring due to winds modified mainly by vertical transport of energy by water vapor, possibly by some horizontal transport by winds from low to high latitudes, with lesser effects of absorption and radiation of infrared wavelengths by water vapor and carbon dioxide. The increase of temperature with altitude above the stratosphere to a maximum of about $270^\circ K$ at about 50 km, and its decrease to a cold minimum of about $190^\circ K$ at about 80 km (Fig. 3) has been attributed to the absorption of sunlight by ozone. Although this seems to be almost certainly true, it has never been proved by a rigorous calculation. A complete theoretical treatment of the radiative and heat transfer processes in each level of the atmosphere is very complicated, but might be profitable now that samples of probably all necessary quantities, except perhaps winds or air movements, are known from rocket data.

A number of writers, the most recent being Johnson,[13] have reached interesting conclusions by considering a simplification of the problem, namely, the diurnal temperature changes due to ozone. For each level of the atmosphere Johnson calculated the rate of absorption of energy from sunlight by the Chappuis (4200A to 7500A) and the Hartley (2300A to 2900A) bands of ozone using the solar energy curves of Figs. 5 and 6. This was done for each hour of the day and for the total day. Since rocket data indicated that seasonal temperature variations were less than $\pm 10^\circ C$ (in altitudes from 40 to 100 km, it was assumed that the total heat energy absorbed at each level during the daylight hours each day was lost at a constant rate during the 24 hours of the day by cooling due to infrared radiation from the same level; thus equilibrium was assumed to prevail on a day-to-day basis. The temperature variation throughout the day was then calculated from the known heat capacity at each level. Three of the curves are given in Fig. 12 for altitudes 42, 48, and 70 km for the ozone curve of the June 14, 1949, flight. It is seen that the temperature was a minimum between 0500 and 0700 hours and a maximum between 1700 and 1900 hours, depending on the altitude. The amplitude of the diurnal change at various altitudes, plotted in Fig. 13, was a maximum of $5.6^\circ C$ and $7.5^\circ C$ for the flights of June 14, 1949, and January 25, 1951, respectively. These were not large changes and were in agreement both with the fact that no diurnal change has been observed and with indirect evidence furnished by the constancy of the height of the E layer during the day and night, which indicated that the diurnal temperature changes in the air below 100 km averaged less than 10°.

Fig. 12 - Calculated diurnal temperature variation for three altitudes

The cooling rates required to dissipate the amounts of heat calculated to be absorbed by the observed concentrations of ozone are shown as a function of altitude in Fig. 14. The temperature distribution is also plotted in Fig. 14, and since the altitude of maximum temperature agrees with the altitude of maximum cooling, it may be concluded that the high temperature at this altitude is the cause of the large cooling rate there. Further, since the concentration of ozone relative to the air is generally a

Fig. 13 - Height distribution
of calculated amplitude of diur-
nal temperature variation
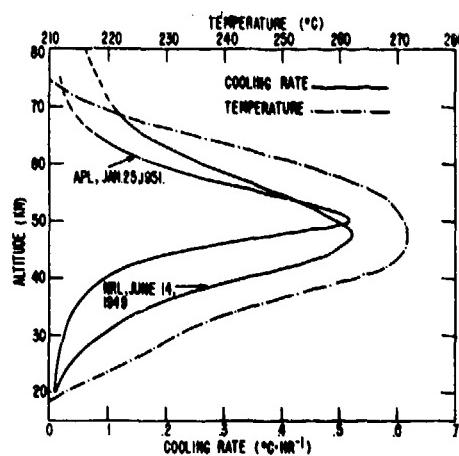
Fig. 14 - Calculated cooling rates

maximum at about 30 km, which is lower than the 50-km altitude of the temperature maxi-
mum, it follows that ozone is not the principal radiator; if it were, the maximum cooling
effect would be below the temperature maximum, perhaps near 40 km. It appears probable
that carbon dioxide or water vapor or both must be the most important causes of the loss
of energy at these altitudes.

7. DISSOCIATION OF OXYGEN IN THE
UPPER ATMOSPHERE

If a gas in the atmosphere absorbs at certain wavelengths emitted by the sun, and if
no other atmospheric gas which absorbs at these wavelengths is present, its density---
or number of particles per unit volume (cu cm)--- at various altitudes may be determined
from the energy in the specified wavelengths observed at the various altitudes. This was
done [7,14] by means of photon counters on rockets for two cases at altitudes from 100 to
128 km: (a) for the total gases of the atmosphere and (b) for molecular oxygen. In the
first case a photon counter sensitive to a band of x-rays, 44A to 51A, was used for which
the absorption cross section of air was 2.2 to 3.0×10^{-18} cm^2. And in the second case a
photon counter was used sensitive to a band of ultraviolet, 1425 to 1500A, near the center
of the great Hartley band of molecular oxygen for which the absorption cross section was
1.50×10^{-17} cm^2.

Data which were in agreement were obtained on rocket flights of V2 No. 49 and
Aerobees 14 and 16; the results of Aerobee 16, fired on December 1, 1953, were the most
complete and are described here. On this flight the solar intensity was measured with the
45A to 51A x-ray photon counter from 100 to 128 km which gave upper air densities about
1/2 to 1/3 the values of Table 1 in this altitude range. One cannot decide from the data at
hand which is correct. Certainly the x-ray measurement should be repeated for it is very
direct and simple to interpret. It is, however, only useful in the altitude range where the
absorption of the superincumbent air for the x-rays is neither too large not too small.

With the 1425A-1500A ultraviolet photon counter on Aerobbe 16, solar intensities were observed from which the number, n_2, of oxygen molecules per cubic centimeter was determined.[14] The values are given in Table 8. Let n be the total number of particles per cubic centimeter and assume that 0.21 n is the number of oxygen molecules which would exist if none were dissociated. Then the fraction, f, of O_2 which is dissociated is

$$f = 1 - n_2/(0.21n). \qquad (7)$$

Table 8 presents the values of f calculated from Eq. (7) with n from Table 1 and Table 2.

TABLE 8
Density n_2 and Dissociation f of O_2
From X-Ray Measurements

Altitude (km)	Density, n_2 (molecules cm^{-3})	Dissociation, f	
		With n of Table 1	With n of Table 2
110	16.2×10^{10}	0.83	0.62
120	3.0×10^{10}	0.88	0.72
128	1.2×10^{10}	0.95	0.77

Same value used for AEDC Model Atmosphere, 1956 — but their total density chosen is slightly higher than that in Table II this report. *

\11.2\

The conclusion from Table 8 is that from 100 to 128 km, oxygen is considerably but not entirely dissociated (not a very exact conclusion but the best that can be made in view of the uncertainty in the air density). This is in accord with the mass spectrograph result (Table 3) that O and O_2 existed from 98 to 137.3 km, and the ion spectrograph result (Table 4) that O^+ and O_2^+ existed from 94 to 219 km. Therefore, oxygen dissociation of 62, 72, and 77 percent at 110, 120, and 130 km, respectively, was assumed in Table 2, which when extrapolated to great heights indicated that molecular oxygen may exist up to 300 km. This has important consequences. It suggests a larger concentration of O_2 above 100 km than would be expected from photochemical equilibrium, but such as would be expected as a result of diffusive separation and turbulent mixing[15]; O_2 at high altitudes has been assumed to explain the excitation of the oxygen green line 5577A in the night air glow.[16] As shown later (Section 11) the theory of the recombination in the F2 region of the ionosphere depends on the vertical distribution of O_2.

8. THE IONOSPHERE

The ionosphere has become better understood, and some of its irregularities are now not completely enigmatical but are recognized as a pattern of not too important variations overlying a pattern of regularity. Early observations by means of the skip distance of radio waves[17] showed that the ionospheric ionization increased during the day and grew less at night. Therefore it was natural to suppose that the ionization was caused by radiation from the sun. After 1930 many ionospheric stations were put into operation and ionosperic records, continous over the years, were gathered at many locations on the earth.

*From conversation with W.S. Ripley, AEDC Research Lab, on 6 Dec 1957
C. M. Golchosten
LFPL

From the records were derived the critical frequency f_c and the virtual height h' of the
ionospheric regions E, F1, and F2; f_c was related to y_m, the maximum value of the curve
of electron density against height. Information about the D region at 70 to 90 km was
obtained by special long wave experiments,[18] and a portion of region E, characterized by
sudden local appearance of dense ionization night or day, was proved to be due to meteors.[19]

It was found that y_m and h' for normal E and F1 were on the whole quite regular; y_m
varied approximately with $(\cos Z)^{1/2}$, where Z is the solar zenith angle, and h' decreased
with a decrease of Z, as would be expected if solar ultraviolet or x-rays caused the
ionization.

On the other hand y_m and h' of F2 were found to exhibit many complexities. For
example, the diurnal maximum of y_m of F2 occurred near noon in temperate latitudes in
winter, during late afternoon in these latitudes in summer, and during late afternoon in
tropical latitudes at all seasons, the winter values being much greater than the summer
and tropical values. There was a pronounced dip in the noon values of y_m at equinox at
the magnetic equator. The value of y_m of F2 increased about 4 times from sunspot mini-
mum to sunspot maximum, whereas y_m of E and of F1 increased about 1.5 times. At
Washington h' of F2 rose in a few hours from 250 km at dawn to over 400 km in summer
months. At low magnetic latitudes, as Guam and Huancayo, Peru, h' of F2 remained
between 220 and 280 km during the day, and then in the late afternoon rose swiftly to about
400 km at 9 P.M. and by midnight descended to 250 km where it remained for the rest of
the night. To explain the complexities of y_m and h' of F2, various mechanisms were
invoked, such as heating of the F2 region by sunlight causing expansion, winds, diffusion,
electromagnetic mechanical effects, etc. These mechanisms, although probably true to
some extent, left many features unexplained.

A brilliant simplification and clarification was achieved by Ratcliffe[20] when he worked out
from the original records of ionosphere stations the values of $\bar{y}$, the total number of elec-
trons in a 1-sq-cm vertical column through F2 below y_m. (He pointed out that it would, of
course, be more complete to include also the electrons above y_m, but that the necessary
data were not available.) He then found that $\bar{y}$ behaved in quite a regular manner with
respect to the sun and did not exhibit the eccentric behavior of y_m. The result provided
convincing evidence in favor of the hypothesis that F2 ionization was caused by electromag-
netic radiation from the sun. This meant that the anomalies in y_m and h', although extreme
and erratic, were due to relatively minor shifting and warping of the F2 layer caused by
heating, diffusion, and air movements.

The height distribution of the electron density, y, in the ionosphere was observed[21] with
instruments in rockets over New Mexico at about 10 A.M. on September 29, 1949, November
21, 1950, and May 7, 1954. The results are shown in Fig. 15. The range of the instrumen-
tation was not sufficient to record the relatively low density ($y < 10^4$) of ionization of D
region from 70 to 90 km. The first two flights reached 140 and 160 km, respectively. The
1954 flight reached 200 km, with good data during both the ascent and the descent; in this
case E and F1 regions were traversed and F2 was just entered. At the time of the flight,
a nearby ionosphere station observed the f-h' curve which gave h' = 460 km at 4.6 kc and
f_oF2 = 4.8 Mc, equivalent to y_m = 2.86×10^5 electrons cm^{-3}. Extrapolating the curve to
a maximum of 2.8×10^5 at 280 km, as shown in the dotted curve of Fig. 15 above 220 km,
produced an F2 region which gave the observed value of h' = 460 km. The dotted curve,
although an extrapolation, is the nearest approach to a direct observation of the electron
distribution in F2 which has yet been made. It offers an illustration of how misleading an
idea of the true height of F2 one may obtain from the virtual height measurement, the one
being 280 km and the other 460 km in this case.

It is clear from Fig. 15 that the ionosphere is a heavily ionized continuum extending
throughout the upper atmosphere, and is not separated into distinctly marked layers. The

E, F1, F2, and, probably, D regions are merely
places where the gradients of the y-h' curve
becomes steeper. Relatively slight variations
in the gradients are sufficient to account for
large changes in the virtual heights, and for
considerable changes in y_m while $\bar{y}$ remains
on the whole little changed. Although this had
been realized for many years, it was not too
certain, and one was never sure how much of
a vertical rise and fall of an ionized region
indicated by virtual height changes was real and
how much was refractive mirage. Now it seems
probable that most of such .otions indicated
by virtual height variations are mirage effects
and are not real.

Fig. 15 - Electron density observed
in rocket flights at about 10 A.M. on
September 29, 1949, November 21,
1950, and May 7, 1954. Dotted curve
above 220 km derived from iono-
sphere record.

9. THE D REGION IONIZATION

The D region of the ionisphere is a rela-
tively low density region of ionization at about
70 to 90 km altitude; it was discovered, and
some of its properties were measured, by
means of experiments with reflections of 16 kc (18.7 km) radio waves.[22] Its electron den-
sity was about 300 electrons cm^{-3} in the day and decreased and became unobservable about
two hours after sunset. The height of reflection fell from about 85 to 70 km from dawn to
noon and rose again to 85 km at sunset in the manner to be expected from the variation in
penetration of monochromatic radiation as a function of the zenith angle of the sun. Ordi-
narily the height-time curve was free from fluctuations of more than 1/2 km and was repeated
within 1 km from day to day. These facts indicated a very stable monochromatic source
of D layer ionization.

Rocket measurements [23] with photon counters furnished evidence that the normal D
layer was caused by hydrogen L α (1216A) radiation from the sun. For it was found that
the intensity of L α was 0.1 erg cm^{-2} sec^{-1} for a quiet sun and that this radiation penetrated
the atmosphere through a narrow window in the O_2 absorption spectrum and produced a
maximum rate of ionization at 77 km. Just what ionizing reactions occurred was not known,
but ionization of NO and of O_2 have been suggested.[24] If L α caused the normal D layer,
which is a very steady layer, the solar emission of Lα must be very uniform.

An interesting anomaly discovered in the D region[22] consisted in a sudden lowering
of the height with the onset of a solar flare. The anomaly was investigated recently for
the purpose of learning more about solar flares.[25] The average drop in height was about
4 km for most flares and about 16 km for the largest flares; it occurred within 10 minutes
after the peak of the flare and returned to normal within an hour or two. Friedman and
Chubb[23] pointed out that from the standpoint of the atmospheric absorption coefficient the
flare effect might be due to an enhancement of L α or to x-rays as short as 1A-2A gener-
ated during the flare. They obtained evidence in rocket experiments that both effects
occurred, but were unable to arrive at any quantitative conclusions regarding their rela-
tive importance, although on theoretical grounds the x-rays seemed the more effective.
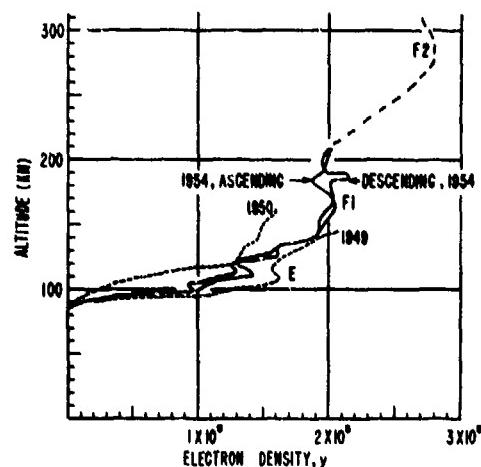
10. NORMAL AND SPORADIC E REGION IONIZATION

The normal E region at about 100 to 130 km altitude has been thoroughly described many times.[26] It is the most regular of the ionospheric regions, it follows solar control very closely, and therefore is caused by solar ionizing electromagnetic radiation, such as ultraviolet light or x-rays. Throughout the day hemisphere, y_m varies with $(\cos Z)^{1/2}$ within 40 percent from 80^0 north to 30^0 south latitude. This means that

$$y_m = y_0 (\cos Z)^{1/2}, \tag{8}$$

where y_0 is the value of y_m for $Z = 0$, i.e., the sun directly overhead. The recombination coefficient, α, is $1 - 2 \times 10^{-8}$; this is rapid, and y_m, being of order 10^5, is reduced by a factor of 10 in a few minutes.

An additional ionization was observed in the E region from 90 to 100 km known as "sporadic" E, or E_S, which is due to causes other than the solar light which produces normal E. A recent study[27] of E_S from 25,000 hourly measurements in 1951 to 1953 at Slough, England, showed that E_S was largely caused by meteors; whether there were any E_S echoes which were not caused by meteors was left undecided. The E_S echoes were characterized by a low reflection coefficient and intermittent appearance; no cases were encountered in which they obscured reflections from or above the normal E region. Over the range of frequencies for which the echoes were observed, the height of reflection was extraordinarily uniform and no group retardation effects were ever observed. Because of rapid recombination, the normal E disappeared soon after sunset, and the only E ionization observed during the night was of the sporadic type.

Sporadic E is due to patches or small clouds of dense ionization which appear and disappear with continually shifting distribution. The E_S echoes were recorded over 85 percent of the time with little seasonal or diurnal variation. Magnetic disturbance, sunspots, or solar flares had no apparent influence on the number of echoes recorded. At oblique incidence the intermittent character of the individual bursts of ionization disappeared and the layer appeared to be more homogeneous. It was a useful layer for certain types of radio communication.

Connected with the effects of meteors observed in the E_S ionization, there is the larger question of possible effects of interplanetary dust and gases on the physics of the upper atmosphere. A comprehensive survey of interplanetary and cosmic dust is given in a volume[28] of papers presented at a symposium in Liége on July 15-17, 1954. A daily deposit on the earth of 10^9 to 10^{10} grams of dust material was mentioned (Ref. 28, page 174), and densities of 300 to 800 electrons per cu cm near the earth's orbit were spoken of. Accretions of such material in the atmosphere would be expected to produce observable effects. At the present time such effects have not been positively identified, except in the case of E_S mentioned above, but their possibility must be kept in mind.

11. THEORY OF E AND F2 REGIONS

By extrapolating the data of the upper atmosphere and of the solar spectrum obtained in the rocket experiments it was possible to work out for the first time a fairly adequate explanation of the E and F2 regions of the ionosphere.[29] The cause of E was attributed to wavelengths shorter than about 100A, of the ionization between E and F2 to wavelengths from about 100A to 200A, and of F2 to the resonance lines of helium, 304A and 584A, with perhaps other solar emissions in the unexplored spectrum from 100A to 977A. The solar spectrum shown in the full-line curve of Fig. 16 was assumed and was based on the observed intensity from 6A to 100A, of Table 5, and on the theory of Elwert[30] of the coronal mechanism

responsible for the emission of x-rays and short ultraviolet wavelengths. An amount of energy $0.05\ \mathrm{erg\ cm^{-2}\ sec^{-1}}$ was assigned to the wavelengths below 50A, 0.05 to the helium continuum ($\lambda < 228A$), and 0.05 to the helium resonance lines 304A and 584A. In the dashed curve of Fig. 16 is given the absorption cross section β_λ for the atmospheric gases from laboratory measurements.

If $i_{0\lambda}$ is the solar energy at wavelength λ falling on top of the atmosphere, the value i_λ at an altitude h is

$$i_\lambda = i_{0\lambda}\ e^{-\beta_\lambda N \cos Z} \qquad (9)$$

where N is the total number of air particles above h in a 1-sq-cm vertical column. The amount of energy absorbed per cubic centimeter per second at h is $\beta_\lambda n i_\lambda$, where n is the air particle density at h, and the number, q_λ, of ion electron pairs produced per cubic centimeter per second at h is

$$q_\lambda = \beta_\lambda n i / \chi \qquad (10)$$

Fig. 16 - Solid line curves, solar energy; dashed curves, atmospheric absorption cross section, β_λ.

where χ is the ionization potential of the air particle, assuming that all the absorbed energy produces ionization. For all air particles, χ was taken to be 4.8×10^{-11} erg (30 ev). From Eq. (9) and (10), n from Table 2, i_λ, and β_λ from Fig. 16, q_λ was calculated and summed over all wavelengths to give q, the total rate of electron production per cubic centimeter at each altitude. The q-h curve is plotted in the dashed-line curve of Fig. 17 which is the sum of curves 1 and 2; these in turn are the sum-curves for the wavelengths of Fig. 16, respectively, less and greater than 200A. The values of q are also listed in Table 9.

From the diurnal variations of y_m of E and $\bar{y}$ of F2, and from solar eclipse variations, the effective recombination coefficients α of E and F2 were calculated[29] to be 1 to 2×10^{-8} and 7×10^{-11}, respectively.

In the atmosphere above 100 km there are two processes which are important in controlling the rate of removal of electrons.[31]

Dissociative recombination

$$e + O_2{}^+ \to O^+ + O,\ \alpha = 3 \times 10^{-8}\ \mathrm{cm^{-3}\ sec^{-1}}, \qquad (11)$$

Photorecombination

$$e + O^+ \to O + h\nu,\ \alpha = 1.5 \times 10^{-12}\ \mathrm{cm^{-3}\ sec^{-1}}. \qquad (12)$$
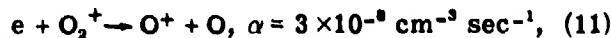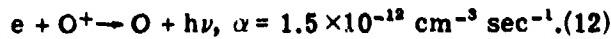
The values of α are approximate theoretical values[31] and are neither in exact agreement with $\alpha = 1$ to 2×10^{-8} observed for E nor with 7×10^{-11} observed for F2. However, Bates and Massey[32] pointed out that atomic ions are rapidly converted to molecular ions by the

Fig. 17 - Theoretical curves of electron production rate, q, and density, y

TABLE 9
Theoretical Values of Ionization Quantities

Altitude, h (km)	Rate of Production, q	Effective Recombination, α	Electron Density, y
100	290	1.5×10^{-8}	1.4×10^{5}
120	400	1.6×10^{-8}	1.6
130	420	1.8×10^{-8}	1.5
150	230	1.6×10^{-8}	1.2
200	80	2.0×10^{-9}	2.0
250	18	1.3×10^{-10}	3.7
300	3.1	1.6×10^{-11}	5.6
350	1.6	3.5×10^{-12}	6.8
400	0.67	1.8×10^{-12}	6.1

charge-exchange process

$$O^+ + O_2 \rightarrow O_2^+ + O, \qquad (13)$$

with a cross section of at least 10^{-17} cm^2. According to Table 2 there are both O and O_2 from 100 to 300 km and therefore the disappearance of electrons depends on all three processes. The effective α was calculated for each height h from Eqs. (11), (12), and (13) using the densities of O and O_2 and the temperature from Table 2. In the calculations, which are not given here, atomic nitrogen was assumed to be equivalent to atomic oxygen. In E levels, because of the abundance of O_2, α depended mainly on dissociative recombination modified slightly by charge exchange. In F2 levels, where the proportion of O_2 relative to O was small but not zero, α was controlled by charge exchange. Above this where there was no O_2 (or N_2), photorecombination was the only process. The resulting values of α are shown in Table 9. It is seen that from 100 to 150 km, α was equal to the observed value for E region. Above 150 km, α decreased very rapidly to the observed F2 value at 280 km and approached the photorecombination value asymtotically at higher altitudes.

Assuming photoelectric equilibrium, and equating the rate of production of electrons to their rate of loss, one has

$$q = \alpha y^2 \qquad (14)$$

The values of y were calculated from Eq. (14) with α and q from Table 9 and are shown in Table 9. These values are also plotted in Fig. 17 and are seen to indicate E and F2 regions in approximate agreement with the observed curves of Fig. 15. It should be noted that the observed curves were for 10 A.M. at latitude 32° north, whereas the theoretical curve refers to the sun directly overhead for sunspot minimum. The theoretical curve has no bump or change of slope at F1 because the necessary details for the explanation of F1 were not known and were not introduced into the theory. The theoretical curve is a static equilibrium curve and may be modified by the rotation of the earth under the sun, and by diffusion, winds, or other influences.

For E and F1, where dissociative recombination controls, Eq. (14) is approximately true, and hence from Eq. (10) the intensity of the solar radiations which cause E and F1 is proportional to y^2. However, for F2, because charge exchange controls, $\alpha \sim 1/y$ and hence Eq. (14) becomes

$$q = by. \tag{15}$$

In this case the intensity of the solar radiations which cause F2 is proportional to y.

At Khartoum, Sudan, during the total solar eclipse of February 25, 1952, Minnis[33] carried out ionospheric measurements which verified certain features of the foregoing theory. In the first place both E and F1 changed in such a way as to be explained by a greatly enhanced (30 times) small region of emission near the west limb of the sun, showing that the locations of the radiation sources for the two layers were the same. Secondly, α was 1.5×10^{-8} for E and 8×10^{-9} for F1 at 170 km, which agrees with Table 9. Thirdly, in the lower part of F2 below the maximum from 200 to 300 km, referred to as F1-1/2, the ionization changed during the eclipse as if α were fairly high (no numerical value was derived), whereas at the maximum of F2 at 350 km α had a much lower value. This agrees with Table 9, although the actual altitudes did not match well because the altitudes of Table 9, being based on various extrapolations, cannot be regarded as definitely determined.

12. ANOMALIES OF THE F2 REGION

The anomalies of the F2 region, which have already been mentioned a number of times, are shown in the contour plots of Figs. 18a, b, c, and d. These are contours of the critical frequency f_0F2 for solstice and equinox for the years 1943-44 and 1947, which were sunspot minimum and maximum, respectively. The plots were prepared by Miss B. Hardwick for D. F. Martyn[34] and were based on the smoothed data[35] of 64 ionosphere stations scattered over the earth. Values of y_m are given by

$$y_m = 1.24 \times 10^{-8} (f_0F2)^2, \tag{16}$$

and it is seen from Fig. 18 that their complexities show a definite pattern related to the magnetic equator of the earth.

Similar world-wide plots of h'F2, the virtual heights of F2, have not been published, but Maeda[36] has plotted many features of the virtual height contours.

A theoretical explanation of the F2 anomalies was worked out by Martyn.[34] Although he has published only a brief synopsis, the theory seems unquestionably correct. It is too involved to be described completely here, and would require too great an excursion into the subject of terrestrial magnetism. The theory makes use of the theoretical electrical currents which are supposed to flow in the ionosphere and cause the solar diurnal variations of the earth's magnetic field.[37] As a result of these currents there is a network of emf's in the ionosphere which, acting together with the earth's magnetic field, produces movements and shifts in the vertical and horizontal distributions of the F2 ionization which are in qualitative agreement with the data of Fig. 18. The slow recombination in F2 is favorable to this type of explanation because it permits the ionization to have a long enough life to move considerable distances.

(a) equinox, 1943-44   (b) equinox, 1947

(c) N. solstice, 1943-44   (d) N. solstice, 1947
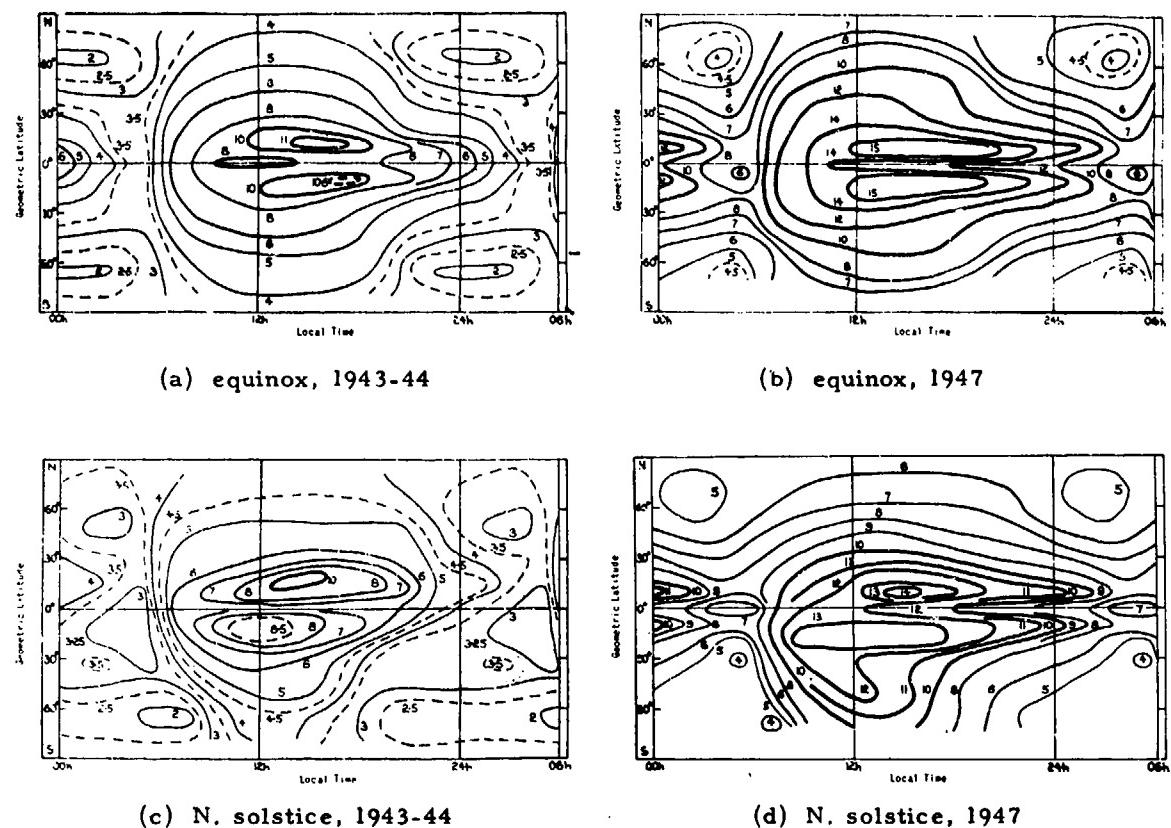
Fig. 18 - Contour plots of critical frequency f_0F2

13. TEMPERATURE AND DENSITY OF THE IONOSPHERE UNDER CONTROL OF THERMAL CONDUCTIVITY

The particle density given by Table 1 is 6×10^9 at 200 km, and an isothermal extrapolation of Table 1 leads to a particle density of order 10^7 at 300 km. There are a number of reasons for believing that such a value is too low, that the temperature above 140 km increases much more rapidly than shown in Table 1 and Fig. 3, and that the density above 200 km is greater than given by an isothermal extrapolation of Table 1. In the first place, large scale heights in F2 levels obtained from ionosphere measurements indicated a temperature of about $1100°K$. Secondly, a particle density of 10^7 at 300 km is so low that there would not be enough air to absorb ionizing radiation from the sun at this level to produce F2. And thirdly, if F2 were produced, diffusion would be so rapid both upward and downward that a stable F2 layer could not exist as high as 300 km, and the F2 layer would be dominated by diffusion, which certainly does not happen.[38]

The only obvious source of heat in the F2 region is the ionizing energy, but calculation showed that the 0.05 erg cm^{-2} sec^{-1}, assumed in Fig. 16 of the F2 theory of section 11, was not sufficient to heat up F2 very much because the thermal conductivity downward was very rapid. Johnson,[39] following an idea of Bates,[40] pointed out that there may be a much larger amount of solar energy than 0.05 erg absorbed in the F2 region which produces "unobserved ionization," which is so quickly destroyed by recombination that it is ordinarily not observed.

As a matter of fact Minnis[33] did observe such ionization in his F1-1/2 region. Furthermore, in the solar spectrum[9] obtained in the rocket flight of February 21, 1955, the Balmer alpha line of He II at 1640A was observed (Fig. 7) and was estimated to contain about 0.006 erg cm^{-2} sec^{-1}. It was reasonable to suppose that there were about 10 times as many Lyman series quanta as Balmer alpha quanta, the energy per quantum being about 5 times greater.

From all this Johnson[39] assumed that the temperature at 300 km was 1100°K, and that the rate of energy absorption was that of components 1 and 2 (Fig. 17) but with component 2, which was the more strongly absorbed, increased by a factor of 15. The thermal conductivity, K at high levels was calculated by assuming (a) that K of O and N was that of a rare gas estimated by interpolating between He and A, (b) that K of a mixture of O, O_2, N, and N_2 was obtained from the respective K's combined according to a linear law, and (c) that $K \sim T^{1/2}$. Then

$$K = 10^6 (3.5 + 0.67\delta) T^{1/2} \text{ cal cm}^{-1} \text{ sec}^{-1} \text{ deg}^{-1}, \tag{17}$$

where δ is the percent dissociation.

The rate of energy absorption at each level was calculated, and the total rate above each level was then obtained by graphical integration. The temperature lapse-rate required to conduct downward the amount of heat absorbed above each level was calculated, and the temperature difference between the isothermal region above 300 km and each level was found. The temperature curve was constructed downward from 1100°K at 300 km. Below about 120 km the temperatures became unreasonably low or negative, showing that conduction alone could not remove the energy rapidly enough. Therefore, below 130 km there was a loss of energy by radiation, probably due to the same radiator which so effectively cools the region near 80 km. Below 130 km the temperature curve was drawn arbitrarily, but low enough to yield a pressure at 120 km in agreement with the x-ray data.[7]

The resulting temperature distribution is shown in curve 3, Fig. 3, and in Table 2. Pressures and particle densities are also given in Table 2. At 120 km the pressure is 1/3 and the particle density 1/2 of those of Table 1; at 220 km they are 3 and 1.2 times those of Table 1, respectively. The model atmosphere of Table 2 should have large diurnal temperature changes above 130 km, but these are difficult to calculate.

14. VARIATIONS OF THE IONOSPHERE AND OF THE SOLAR INTENSITY WITH SUNSPOTS

In order to show the manner in which the ionosphere varied with solar activity, y_0 of E, averaged over the year for the years 1931 to 1954, was calculated from the data[35] of a number of ionospheric stations scattered over the earth. In Fig. 19, y_0 was plotted together with the yearly average Wolf[41] sunspot number s; it is seen that they rise and fall together. A theoretical relation between y_0 and s was derived[26] as follows: From Eq. (14) $y_0 \sim i_0^{1/2}$, where i_0 is the intensity of solar radiation which causes E ionization. Assume that $i_0 \sim (g+s)$, where g is a constant introduced in recognition of the fact that y_0 and i_0 have values other than zero when s = 0, i.e., when there are no sunspots. Then

$$y_0 = f (g + s)^{1/2}. \tag{18}$$

The dashed curve of Fig. 19 was plotted from Eq. (15) with f = 0.154 × 10³ and g = 78.6. It agrees with the observed curve, showing that the Wolf sunspot number is a surprisingly good indicator of the intensity, i_0, of the soft x-rays, or short ultraviolet wavelengths, which cause E region. From sunspot minimum to maximum, y_0 increased by a ratio of 1.5, hence i_0 increased by 1.5² or about 2.3.
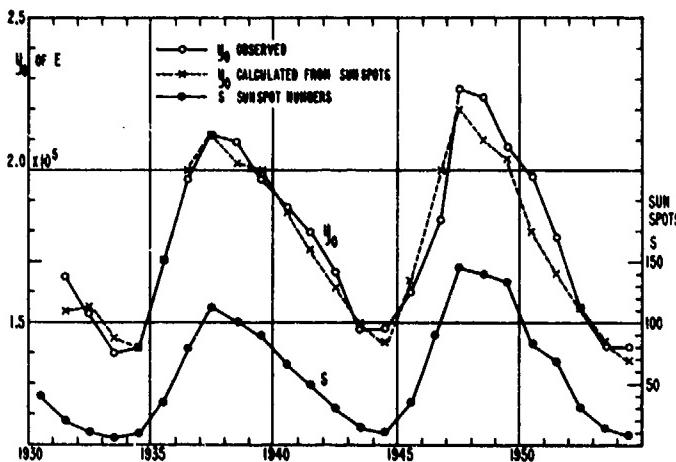
Fig. 19 - Annual mean values of Wolf sunspot
number s; y_0 of E observed and calculated.

The F1 region is known, or exists, only for Z less than about $70°$, because for larger
values of Z, F1 is engulfed, or covered up, by F2 and is concealed from observation. How-
ever, where it is observed, F1 obeys Eq. (8) approximately, and y_0 of F1 is about $2y_0$ of E.
Hence, for F1 Eq. (15) is true with f = 0.3×10^8 and g = 78.6. Thus Fig. 19 is a concise
statement of the major features of y_m of E and F1 throughout all the years that they have
been under routine observation.

On the other hand, as was mentioned earlier, y_m of F2 does not obey Eq. (8) at all,
but varies through the year and over the earth in a very complex manner.[34] However, as
shown by Ratcliffe,[20] the total ionization $\bar{y}$ in a vertical column through F2 below y_m was
fairly regular and increased by a factor of 2 from 1944 to 1939, which was about one year
short of the span from sunspot minimum to maximum. The ionizing energy for F2 there-
fore increased by the same factor, since Eq. (15) holds for F2.

The general conclusion was that from sunspot minimum to maximum in the period
from 1931 to 1954, the solar intensity in all the solar wavelengths which produced E, F1,
and F2 changed by a factor of about 2.3. According to the theory of Section 11 these wave-
lengths are in the region from about 10A to 800A. There are no data on changes in D layer,
or its cause $L\alpha$, over a sunspot cycle. On the other hand, it is known that the intensity of
the longer wavelengths from 3000A to 10,000A does not change by as much as 1 percent
over a sunspot cycle.

15. THE AURORA

Auroras occur in atmospheric levels from about 80 km upward to several hundred km,
and it seems certain that the physical state, as the temperature, pressure, and composition,
of the atmosphere when an aurora is taking place differs considerably from its normal quiet
state. The problem is to determine the cause of the aurora and the state of the atmosphere
when under its influence. At the present time a complete solution of the problem is not in
sight. However, since 1950 some important advances have been made in that the auroral
spectrum has been clarified considerably, evidence has been obtained of protons entering the
auroral region at the commencement of a display, and a new theory of the origin of the
aurora has been proposed.

Meinel, Chamberlain, Petrie, Small, and others[42] obtained improved auroral spectra by means of modern spectrographs of great light-gathering power and considerable dispersion. The spectra were subjected to a more sophisticated analysis than was possible in previous work, and much of the earlier confusion was removed. As a matter of fact the auroral spectrum is very complex, with atomic and molecular emissions well mixed throughout the spectrum and important lines often obscured by strong molecular bands.

The following brief listing is from the paper of Chamberlain and Oliver.[43]

Forbidden Atomic Lines. In general the transition probability of a forbidden line is 10^{-7} to 10^{-9} and less than that of a strong permitted transition. Lines 5577A, 6300A, and 6364A, due to O I, are among the most intense auroral emissions. Line 3727A, due to O II, is weak and its presence is uncertain. Lines 3466A and 5200A, due to N I, are present in moderate intensity. Line 5755A, due to N II, is weak and its existence needs confirmation.

Permitted Atomic Lines. Permitted lines due to O I, O II, N I, and N II are present in the aurora. The D lines of Na I, 5890A, and 5896A, which are strong in the night sky emission, appear faintly in aurora emissions.

Molecular Band Systems. The most prominent band systems in the auroras belong to the neutral and ionized nitrogen molecules. Molecular oxygen systems are quite weak except in auroras that reach well below 100 km, probably because molecular oxygen is scarce above that level. The following band systems are identified: N_2 First Positive, N_2 Second Positive, N_2 Vegard-Kaplan, N_2^+ First Negative, N_2^+ Meinel, O_2 Atmospheric, and O_2^+ First Negative.

Hydrogen Lines. The Balmer lines of hydrogen were observed in auroras by Vegard and his associates as early as 1939, but their identifications were uncertain until confirmed by Gartlein in 1950. The fact that the lines were somewhat broadened was attributed to Doppler motions. In a patrol study of auroral emissions from June 1 to September 20, 1953, by Fan and Schulte[44] at the Yerkes Observatory, it was found that all quiet arcs showed a very intense Hα line, whereas rayed features never showed Hα. Large intensity variations in Hα were noted on plates taken in rapid succession. Some data were obtained which indicated that the auroral hydrogen emissions were stronger in lower magnetic latitudes.

Helium Lines. In early work a number of faint features in the auroral spectrum were ascribed to He I, but later observations indicated that the identifications were doubtful.

Meinel[45] at the Yerkes Observatory made an important advance in auroral physics by the use of small, powerful spectrographs with which he was able to obtain spectra of limited regions of the sky with exposures of only 20 to 40 minutes, and thereby to observe short-lived spectral features of auroral displays which had never been seen before. When the spectrograph was pointed at a quiet auroral arc in the magnetic zenith during the great display of August 18 to 20, 1950, Hα was observed with diffuse Doppler broadening to shorter wavelengths indicating that protons were entering the upper atmosphere at high speeds, the Doppler spread reaching 3300 km sec^{-1}. The protons of course could not emit Hα, but could do so when they had been slowed down sufficiently by collisions to capture electrons into the third Bohr level. Therefore the result was interpreted as indicating that their speeds of approach to the earth were greater than 3.3×10^8 cm sec^{-1}. If it is assumed that the lower boundary of the arc was at 85 km and that this marked the end of the range of the incoming proton, then, from Table 1 or 2, the vertical thickness of air above 85 km is 5 cm (NTP) and to penetrate this thickness a proton speed of 1.2×10^9 cm sec^{-1}, or energy of 750 kev, is required.

At the same time the lines of N_2, N_2^+, and O I, which were also present with Hα in the quiet arc spectrum, had no one-sided Doppler spreading, indicating that these emissions

were secondary results caused directly or indirectly by the reactions of the incoming protons with the particles of the upper atmosphere. The H α emission was concentrated near the bottom of the arc, and decreased with height more rapidly than the other emissions.

When the spectrograph was pointed at the quiet arc on the magnetic horizon the Doppler broadening of H α was symmmetrical about a zero velocity in the line of sight. In Fig. 20 are shown the observed H α profiles.
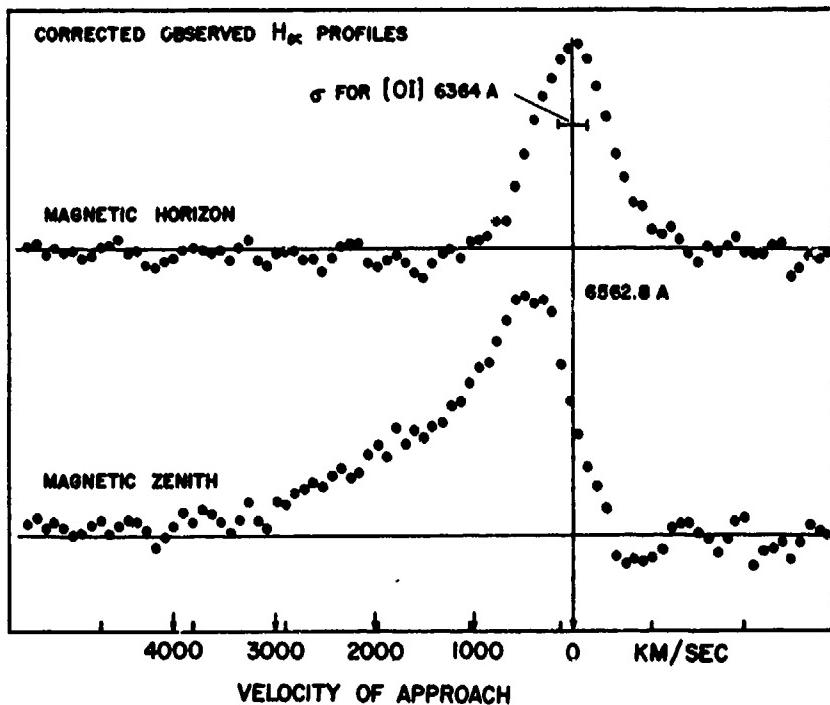
Fig. 20 - Profiles of Hα in the auroral arc of August 19, 1950
(after Meinel, Ref. 45)

Further observations indicated the following pattern of events in an auroral display. The presence of the quiet auroral arc with strong Hα emission was characteristic of the commencement of the display. After a time, which varied from minutes to hours in different displays, the quiet arc broke up, coinciding with the abrupt ending of Hα emission, and the rapidly changing luminous features of the display set in, such as rays and flaming clouds, as if the incoming protons were the primary excitation source, and the rays and flaming structures were after-effects. Why the region above an arc suddenly becomes active and produces a ray structure and clouds of luminosity is still a mystery.

The Yerkes group attempted to reproduce in the laboratory spectra similar to those of the aurora by shooting beams of charged particles into air at a pressure of about 10^{-1} mm of Hg, which corresponds to an altitude of about 65 km. With H^+ and He^+ at energies in steps from 40 to 400 kev, and with H^+ up to 1.9 Mev, it was found[46] that the laboratory spectra bore a close resemblance to the auroral spectrum, except that the infrared N_2^+ Meinel bands were much too weak relative to the N_2 First Positive Bands. There were other differences: for example, NO bands were strong in the laboratory discharges, but were not observed in the aurora. In subsequent experiments[47] it was found that 0.2 to 7 kev electrons were the only particles which were able to excite the N_2^+ Meinel bands

efficiently. It was pointed out that such electrons could not possibly enter from the top of the atmosphere and penetrate to auroral levels. Therefore it was concluded that the electrons, if they existed, must be of secondary origin, caused somehow by the incoming protons or other heavy particles.

On the theoretical side Chamberlain[48] has contributed important ideas, dealing first with the homogeneous auroral arc and then with the auroral rays. In the case of the arc, when a beam of protons was assumed all coming down in the same direction along a line of magnetic force, the calculated distribution with altitude of H α turned out to be in a thin layer, only a few km in thickness, which did not agree with the observed spread of the luminosity from about 100 to 140 km. If, however, a dispersion in direction of the protons were assumed, as if they followed spirals of varying pitch along the magnetic line, agreement with observation could be secured. On the other hand a ray appeared to be due to a process fundamentally different from that of the arc, because the ray emitted no hydrogen lines and its luminosity was nearly constant over a density range of more than 100, or an altitude range of more than 50 km. By assuming an electric field of order 1 volt per km in the upper atmosphere along the magnetic lines, Chamberlain[49] obtained a calculated luminosity along the ray in agreement with observation. Whether such electric fields exist has not yet been demonstrated, but Wulf[50] has developed the idea that electric fields would be generated by horizontal winds of the ionosphere moving across the vertical component of the magnetic field.

16. MAGNETIC SELF-FOCUSED SOLAR ION STREAMS AS THE CAUSE OF AURORAS

The auroral theory of Birkland,[51] proposed in 1896 and developed later in mathematical detail by Störmer,[51] assumed that the sun projected toward the earth a stream of particles — electrons or ions — all charged with the same sign, which were diverted to high latitudes by the magnetic field of the earth. Schuster[51] pointed out that the electrostatic repulsion of the particles would disperse the stream long before it reached the earth. To get around this difficulty, Bennett and Hulburt[52] invented a new theory based on magnetic self-focusing effects of ionized streams. These effects, which were worked out in some detail by Bennett[53] in 1934, modify and counteract the electrostatic spreading effects in such streams. In the theory it was assumed that the sun emits a conical stream of high-speed positive ions (either protons or other types of ions) and negative electrons in equal numbers and, at first, of equal speeds. The free path of a charged particle through a completely ionized gas depends approximately on the fourth power of the speed and the square of the mass of the particle. Therefore as the stream passes out through the ionized atmosphere of the sun (the corona), the electrons experience many more collisions than the ions and are slowed up or thrown out of the stream. But, because of electrostatic forces the electrons are continually replaced in the stream from the slow electrons of the surrounding ionized gas. The stream of positive ions continues and constitutes an electric current, but at all times all parts of the stream and the surrounding gas are closely (but not exactly) electrostatically neutral. Due to the magnetic field of the electric current, the fast-moving positive ions are continually compressed into the stream, and the electrons and the slower positive ions are continually ejected from the stream. This is termed 'magnetic self-focusing.' The stream develops into a narrow core of fast-moving positive ions which progresses through space and, if correctly aimed, enters the influence of the earth's magnetic field and is diverted to auroral latitudes. The stream is pictured in Fig. 21.

Now, if the space between the sun and the earth were a vacuum, the stream of positive ions would be quickly dispersed by electrostatic repulsion and would cease to exist. Therefore the theory required that the space between the earth and the sun be filled with an ionized gas, and that the density of the gas be greater than a certain lower limit which depends upon

Fig. 21 - Magnetic self-focused
ion stream of auroral theory

the strength of the electric current of the stream. Calculation showed that for a positive ion current which carried an energy equal to that of an auroral display, the density of ion-electron pairs in the space between the earth and the sun must be greater than about 10^{-2} cm^{-3}. A density of ionization of this amount, and even up to five orders of magnitude greater, appeared to be open to no objection. But its existence cannot be said to have been proved by experiment, and it therefore remains at present an essential hypothesis of the theory.

The system comprised of the sun, the earth, and the intervening space is a stable electrical system. The loss of positive charge from the sun in the fast auroral ion stream, and the gain by the earth, is compensated by a slow drift of positive space ionization to the sun, and of negative space ionization to the earth.

The self-focused stream theory inherited a long standing difficulty of the Birkland-Störmer theory. To explain this let us assume that the lower boundary of the auroral arc was at 85 km and that this marked the end of the range of the incoming protons. The vertical thickness of the air above 85 km is 5 cm (NTP), and to penetrate this thickness a proton speed of 1.2×10^9 cm sec^{-1} is required. However, the calculations of Störmer have shown that a proton must approach the earth with a speed of 10^{10} cm sec^{-1} in order to reach the zone of maximum auroral frequency at magnetic latitude 65° to 70°; with such speeds the proton range in air is 25 meters, and the protons would plunge down to an altitude of about 40 km before being stopped. Several suggestions were made[52] to explain away the difficulty, the simplest depending on the fact that the Stormer calculation referred to a single charged particle, whereas an electric current has a greater magnetic stiffness than the particles of which it is composed. However, the exact calculation of the bending of a current of particles by the earth's magnetic field is difficult and has never been made. Therefore at the present time the importance of the above difficulty is not known.

17. CONCLUDING REMARKS

Further progress in investigating the upper atmosphere may be expected in the immediate future. The Yerkes Observatory is pursuing its study of auroral and night sky spectra and their reproduction in the laboratory. At the University of Cambridge, England, the use of radio pulse techniques is being exploited vigorously as a means of studying the changes, irregularities and other phenomena of F2 ionization. The Naval Research Laboratory plans to continue its rocket program by developing the "Aerobee High" rocket. This is the Aerobee rocket with strengthened design and increased power which should enable it to reach an altitude of 250 km and perhaps even 300 km. If this rocket becomes available it will serve as a vehicle for investigating the atmosphere above 200 km well into the main F2 region, a region which has not been well explored.

In addition to results expected from these separate, relatively small endeavors, a great advance in knowledge of the upper atmosphere and its associated phenomena appears certain to result from the experiments which are being planned for the period of the International Geophysical Year from July 1957 through December 1958. About 40 nations in cooperation are organizing a large and intensive experimental program which is to be carried out during this time on a world-wide scale.

* * *

REFERENCES

1. Newell, H. E., "Rocket Data on Atmospheric Pressure, Temperature, Density and Winds," Ann. de Géophys., 11:115-144 (1955). A survey paper with bibliography.

2. The Rocket Panel, "Pressures, Densities and Temperatures in the Upper Atmosphere," Phys. Rev., 88:1027-1032 (1952)

3. Maris, H. B., "The Upper Atmosphere," Terr. Mag. and Atmos. Elec., 33:233-255 (1928); 34:45-53 (1929)

(4) Towsend, J. W., Meadows, E. B., and Pressly, E. C., "A Mass Spectrometric Study of the Upper Atmosphere," Rocket Exploration of the Upper Atmosphere, p. 169-188, R. L. F. Boyd and M. Seaton, Ed., New York:Interscience (1954).

5. Johnson, C. Y., and Meadows, E. B., "First Investigation of Ambient Positive Ion Composition to 219 km by Rocket Borne Spectrometer," J. Geophys. Res., 60:193-203 (1955)

6. Johnson, F. S., Purcell, J. D., Tousey, R., and Wilson, N., "The Ultraviolet Spectrum of the Sun," Rocket Exploration of the Upper Atmosphere, p. 279-288, R. L. F. Boyd and M. J. Seaton, Ed., New York:Interscience, (1954). A survey paper with bibliography

7. Friedman, H., "The Solar Spectrum Below 2000 Angstroms," Ann. de Géophys., 11:174-180 (1955). A survey paper with bibliography.

8. Durand, E., Oberly, J. J., and Tousey, R., "Analysis of the First Rocket Ultraviolet Solar Spectra," Astrophys. J., 109:1-16 (1949); Wilson, N. L., Tousey, R., Purcell, J. D. Johnson, F. S., and Moore, C. E., Astrophys. J., 119:590-612 (1954).

9. Johnson, F. S., Malitson, H. H., Purcell, J. D., and Tousey, R., "Emission Lines in the Solar Ultraviolet Spectrum," Astrophysical J. In press.

Johnson, F. S., "Rocket Observations of Atmospheric Ozone," Proc. Meteor. Conf. Toronto, p. 17-26 (1953). A survey paper with bibliography.

1. Johnson, F. S., Purcell, J. D., Tousey, R., and Watanabe, K., "Direct Measurements of the Vertical Distribution of Atmospheric Ozone to 70 Kilometers Altitude," J. Geophys. Res., 57:157-176 (1952)

12. Hulburt, E. O., "Explanation of the Brightness and Color of the Sky, Particularly the Twilight Sky," J. Opt. Soc. Amer., 43:113-118 (1953)

13. Johnson, F. S., "High Altitude Diurnal Temperature Changes Due to Ozone Absorption," Bull. Am. Meteor. Soc., 34:106-110 (1953)

14. Byram, E. T., Chubb, T. A., and Friedman, H., "Dissociation of Oxygen in the Upper Atmosphere," Phys., Rev., (1955). In press.

15. Nicolet, M., and Mange, P., "The Dissociation of Oxygen in the High Atmosphere," J. Geophys. Res., 59:15-45 (1954)

16. Nicolet, M., "Origin of the Emission of the Oxygen Green Line in the Airglow," Phys. Rev., 93:633 (1954)

17. Hulburt, E. O., "Ionization in the Upper Atmosphere of the Earth," Phys.,Rev., 31:1018-1037 (1928).

18. Best, J. E., Ratcliffe, J. A., and Wilkes, M. V., "Experimental Investigation of Very Long Waves Reflected from the Ionosphere," Proc.,Roy. Soc., 156:614-633 (1936)

19. Appleton, E. V., and Naismith, R., "The Radio Detection of Meteor Trails and Allied Phenomena," Proc. Phys. Soc. Lond., 59:461-472 (1947)

20. Ratcliffe, J. A., "Some Regularities in the F2 Region of the Ionosphere," J. Geophys. Res., 56:487-507 (1951)

21. Seddon, J. C., Pickar, A. D., and Jackson, J. E., "Continous Electron Density Measurements up to 200 km," J. Geophys. Res., 59:513-524 (1954)

22. Budden, K. G., Ratcliffe, J. C., and Vilkes, M. J., "Further Investigations of Very Long Waves Reflected from the Ionosphere," Proc. Roy. Soc., 171:188-214 (1939)

23. Friedman, H., and Chubb, T. A., "Solar X-Ray Emission and the Height of D Layer During Radio F de-Out," Cambridge Conference Physics of the Ionosphere, p. 58-62 (1954)

24. Mitra, A. P., "The D Layer of the Ionosphere," J. Geophys. Res., 56:373-402 (1951). A survey paper with bibliography.

25. Bracewell, R. N., and Straker, T. W., "The Study of Solar Flares by Means of Very Long Radio Waves," Monthly Notices Roy. Astron. Soc., 109:28-45 (1949)

26. Hulburt, E. O., "The E Region of the Ionosphere," Phys. Rev., 55:639-645 (1939)

27. Naismith, R., "A Subsidiary Layer in the E Region of the Ionosphere," J. Atmos. and Terr. Phys., 5:73-82 (1954)

28. Swings, P., Ed., "Les Particules Solide dans les Astres," Mém. Soc. Roy. Sci. de Liége., Sér. 4, Vol. 15 (1955)

29. Havens, R. J., Friedman, H., and Hulburt, E. O., "The Ionospheric F2 Region," Conference on the Physics of the Ionosphere, Cambridge, September 1954, p. 237-244, Phys. Soc. London (1955)

30. Elwert, G., "The Continuous Emission Spectrum of the Solar Corona in the Far UV and the Adjacent X-Radiation," Z. Naturforsch., 7a:202-204 (1952)

31. Bates, D. R., Buckingham, R. A., Massey, H. S. W., and Unwin, J. J., "Dissociation, Recombination and Attachment Processes in the Upper Atmosphere," Proc. Roy. Soc. A, 170:322-340 (1939)

32. Bates, D. R., and Massey, H. S. W., "The Basic Reactions in the Upper Atmosphere. II - The Theory of Recombination in the Ionized Layers," Proc. Roy. Soc. A, 192:1-16 (1947)

33. Minnis, C. M., "Ionospheric Behaviour at Khartoum during the Eclipse of 25th February 1952," Atmos. and Terr. Phys., 61:91-112 (1955)

34. Martyn, D. F., "Geomagnetic Anomalies of the F2 Region and Their Interpretation," Conference on the Physics of the Ionosphere, Cambridge, September 1954, p. 260-264, Phys. Soc. London (1955)

35. "Ionospheric Data," Central Radio Propagation Laboratory, U. S. National Bureau of Standards.

36. Maeda, K., "Geomagnetic Distortion in the F2 Layer," Conference on the Physics of the Ionosphere, Cambridge, September 1954, Phys. Soc. London (1955)

37. Bartels, J., "Some Problems of Terrestrial Magnetism," Terrestrial Magnetism and Electricity, Fleming, J. A., Ed., Chapter 8, p. 385, New York:McGraw Hill (1939)

38. Martyn, D. F., "Theory of Height and Ionization Density Changes at the Maximum of a Chapman-Like Region Taking Account of Ion Production, Decay, Diffusion and Tidal Drift," Conference on Physics of the Ionosphere, Cambridge, September 1954, p. 260-264, Phys. Soc. London (1955)

39. Johnson, F. S., "Temperature Distribution of the Ionosphere under Control of Thermal Conductivity," J. Geophys. Res., In press.

40. Bates D. R., "The Temperature of the Upper Atmosphere," Proc. Phys. Soc. London, B, 64:805-821 (1951)

41. "Wolf's Sunspot Numbers, Annual Mean," Smithsonian Physical Tables, Ninth Revised Edition, Table 824, p. 727 (1954)

42. Chamberlain, J. W., and Meinel, A. B., "Emission Spectra of Twilight, Night Sky and Aurorae," The Earth as a Planet, Chapter 11, Edited by G. P. Kuiper, The University of Chicago Press (1954). A survey paper with biobligraphy.

43. Chamberlain, J. W., and Oliver, N. J., "Atomic and Molecular Transitions in Auroral Spectra," J. Geophys. Res., 58:457-472 (1953)

44. Fan, C. Y., and Schulte, D. H., "Variations in the Auroral Spectrum," Astrophys. J. 120:563-565 (1954)

45. Meinel, A. B., "Doppler-Shifted Auroral Hydrogen Emission," Astrophys. J. 113:50-59 (1951)

46. Meinel, A. B., and Fan, C. Y., "Laboratory Reproduction of Auroral Emissions by Proton Bombardment," Astrophys. J. 115:330-331 (1952)

47. Fan, C. Y., "The Possible Role of Accelerated Secondary Electrons in the Aurora," Astrophys. J., 119:294-295 (1954)

48. Chamberlain, J. W., "On the Production of Auroral Arcs by Incident Protons," Astrophys. J., 120:566-571 (1954)

49. Chamberlain, J. W., "Theory of Auroral Rays," J. Atmos. and Terr. Phys., Supplement 3: The Airglow and Aurora (1956)

50. Wulf, O. R., "On the Production of Glow Discharges in the Ionosphere by Winds," J. Geophys. Res., 58:531-538 (1953)

51. Ferraro, V. C. A:, "The Aurorae," a recent review in "Advances in Physics," a supplement of the Phil. Mag., 2:265-320 (1953)

52. Bennett, W. H., and Hulburt, E. O., "Theory of the Aurora Based on Magnetic Self-Focusing of Solar Ion Streams," Phys., Rev., 95:315-319 (1954); "Magnetic Self-Focused Solar Ion Streams as the Cause of Aurorae," J. Atmos. and Terr. Phys., 5:211-218 (1954).

53. Bennett, W. H., "Magnetically Self-Focusing Streams," Phys.,Rev., 45:890-897 (1934)

* * *

UNCLASSIFIED

Naval Research Laboratory. Report 4600. ADVANCES IN THE PHYSICS OF THE UPPER AIR SINCE 1950. by E. O. Hulburt. 33 pp. 8 figs. October 25, 1955.

The report describes progress which has been made since about 1950 in investigating the upper atmosphere. Important data up to great heights were obtained by means of instruments on rockets. The vertical distribution of atmospheric density was measured to 219 km, of pressure to 130 km, of ozone to 70 km, and of electron density to 219 km. In a daytime flight O_2, O, O_3, and N were observed from 90 to 137 km; O_2 was observed to be more than 60 percent dissociated from 110 to 128 km. The ratio A/N_2, argon to molecular nitrogen, was found to be about the same from 110 to 137 km as at ground level. Positive ions of atomic masses 16, 26, 30, and 32, identified as O^+, C^+, NO^+, and O_2^+, respectively, were observed in a daytime flight from 94 to 128 km. In a night flight only O_2^+ was recorded from 97 to 118 km. From an altitude above 100 km the solar spectrum was photographed into the vacuum ultraviolet to 970A, and was recorded with photocells in the soft x-ray region from 100A to 6A. At about 2090A the character of the spectrum changed abruptly, the energy decreased sharply, the Fraunhofer absorption lines disappeared and at shorter wavelengths gave way

UNCLASSIFIED   (over)

1. upper atmosphere research
2. upper atmosphere — physical properties
I. Hulburt, E. O.

to emission lines. The vertical distribution of ozone was measured to 70 km, and a quantitative theory of ozone formation was worked out. Calculation indicated that the temperature maximum at about 50 km was due to the absorption of solar ultraviolet energy by ozone. The various facts of the ionosphere were gathered together in a theory which attributed the cause of the normal D region to solar hydrogen Lyman α, 1216A, of normal E region to x-rays below 100A, and of F2 to ultraviolet light in the thus far unobserved spectrum from 200A to 600A. No explanation of F1 was made. Anomalies in D ionization appeared to be due to enhanced bursts of solar x-rays, and sporadic E appeared to be blocs of ionization caused by meteors. A working model atmosphere based on the observed pressure, density, and composition was drawn up and extrapolated to 500 km. Its temperature increased rapidly from 200°K at 100 km to 1045°K at 200 km, and 1100°K at 300 km; the temperature was calculated to agree with the energy supplied by the ionosphere and heat conduction downward. From the observed changes in the solar intensity in the ionosphere over two solar cycles, the solar intensity in the wavelengths which cause E, F1, and F2 was calculated to increase by a factor of about 2.3 from sunspot minimum to maximum. Better spectra and better analysis of the spectra removed much confusion about the auroral spectrum. Doppler broadened Hα was discovered in the quiet auroral arc at the commencement of an auroral display, and was interpreted to mean that the display was initiated by solar protons of speeds greater than 3000 km per sec entering the upper atmosphere. A new theory of the aurora was outlined based on magnetically self-focused proton streams from the sun.

Naval Research Laboratory
Technical Library
Research Reports Section

DATE: January 25 2001

FROM: Mary Templeman, Code 5227

TO: **Code 7600 Dr. Gursky**

CC: Tina Smallwood, Code 1221.1 *la 1/25/01*

SUBJ: Review of NRL Reports

Dear Sir/Madam:

1. Please review NRL Report FR-4600 for:

    ☑ Possible Distribution Statement
    ☐ Possible Change in Classification

Thank you,

Mary Templeman

Mary Templeman
(202)767-3425
maryt@library.nrl.navy.mil

The subject report can be:

☑ Changed to Distribution A (Unlimited)
☐ Changed to Classification _____
☐ Other:
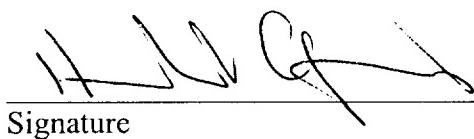
_____   1/25/01
Signature   Date

-- 1 OF 1
-- 1 - AD NUMBER: B183345
-- 2 - FIELDS AND GROUPS: 4/1
-- 3 - ENTRY CLASSIFICATION: UNCLASSIFIED
-- 5 - CORPORATE AUTHOR: NAVAL RESEARCH LAB WASHINGTON DC
-- 6 - UNCLASSIFIED TITLE: ADVANCES IN THE PHYSICS OF THE UPPER AIR
--   SINCE 1950,
-- 8 - TITLE CLASSIFICATION: UNCLASSIFIED
--10 - PERSONAL AUTHORS: HULBURT, E. O.
--11 - REPORT DATE: 25 OCT 1955
--12 - PAGINATION: 36P MEDIA COST: $ 7.00 PRICE CODE: AA
--14 - REPORT NUMBER: NRL-4600
--18 - MONITOR ACRONYM: XB
--19 - MONITOR SERIES: NRL
--20 - REPORT CLASSIFICATION: UNCLASSIFIED
--21 - SUPPLEMENTARY NOTE: SUPERSEDES AD-077 444.
--22 - LIMITATIONS (ALPHA):   DISTRIBUTION: DTIC USERS ONLY.
--23 - DESCRIPTORS: *ATMOSPHERIC DENSITY, *SOLAR ACTIVITY, *UPPER
--   ATMOSPHERE, OZONE, ATMOSPHERIC TEMPERATURE, THERMAL CONDUCTIVITY,
--   IONOSPHERE, F REGION, AURORAE.
--24 - DESCRIPTOR CLASSIFICATION: UNCLASSIFIED
--25 - IDENTIFIERS: N-40550, F2 REGION, POSITIVE IONS
--26 - IDENTIFIER CLASSIFICATION: UNCLASSIFIED

-
--29 - INITIAL INVENTORY: 1
--33 - LIMITATION CODES: 12
--35 - SOURCE CODE: 251950
--36 - ITEM LOCATION: DTIC
--40 - GEOPOLITICAL CODE: 1101
--41 - TYPE CODE: N
--43 - IAC DOCUMENT TYPE: